The Function of Neurogranin in the Regulation of Sodium Channel and NMDA Receptor Channel

ZHOU QUAN (B.Sc., Univ. of Science and Tech. of China)

A THESIS SUBMITTED
FOR THE DEGREE OF MASTER OF SCIENCE
DEPARTMENT OF BIOLOGICAL SCIENCES
NATIONAL UNIVERSITY OF SINGAPORE
2005

ACKNOWLEDGEMENTS

I would like to express my most heartfelt and sincere gratitude to the following people, without whom the completion of this project would not have been possible:

-my supervisor A/P Sheu Fwu-shan for the encouragements, the most valuable guidance and patience throughout the course of the whole project.

-Dr. Han Nianlin for the constant guidance and advice. Her help, stimulating suggestions and encouragement helped me in all the time of research.

- Ms. Liu Xiao, for her help in plasmids preparation.

- Mr. Gui Jingang, Ms. Wenjing and Ms Tay Bee Ling for their support in times of trouble.

- all other lab colleagues.

Especially, I would like to give my special thanks to my wife Xuan whose patient love enabled me to complete this work

I would also thank National University of Singapore for supporting me with a research scholarship through the two and a half-year study.

As a foreigner, I like Singapore, a beautiful country, and Singaporeans, who are very nice.

CONTENTS

LIST OF FIGURES

LIST OF ABBRIVATIONS

Ng	Neurogranin
PKC	protein kinase C
CaMKII	Ca2+/CaM-dependent kinase II
GAP43	growth-associated protein 43
Ca^{2+}	calcium
NO	nitric oxide
IP_3	inositol 1,4,5-trisphophate
PIP_2	phosphatidylinositol 4, 5-bisphosphate
ER	endoplasmic reticulum
DAG	diacylglycerol
SNP	sodium nitroprusside
CaM	calmodulin
$[Ca^{2+}]_i$	intracellular free calcium concentration
kDa	kilo dalton
SDS-PAGE	sodium dodecyl sulfate-polyacrylamide gel electrophoresis
LTP	long-term potentiation
LTD	long-term depression
TetR	the Tet repressor protein
NOS	NO synthase
nNOS	neuronal NO synthase
eNOS	endothelial NO synthase

iNOS	inducible NO synthase
NMDA	N-methyl-D-aspartate
K_D	dissociation constant
PBS	Phosphate Buffer Saline
VGSCs	Voltage-gated sodium channels
TBST	Tris-buffered saline Tween-20

SUMMARY

Neurogranin (Ng), also known as RC3 and P17, is a postnatal expressed brain-specific protein that is selectively expressed high levels in neuronal cell bodies and dendrites. Ng contains a binding domain, IQ motif, for calmodulin (CaM). Recent studies have suggested that CaM directly interacts with both sodium channel and NMDA channel, and in turn regulates the channel kinetics. We report here that the intracellular infusion of a Ng peptide containing unphosphorylated IQ motif substantially modifies the functional properties of endogenous sodium channels in cortical neuron, while another control peptide containing a phosphorylated IQ motif does not. This result verifies that CaM plays a significant role in sodium channel signaling and suggests that the effect of Ng on sodium channel is through Ng-CaM complex. In contrast, both two Ng peptides have no specific effect on recombinant NMDA receptor channels expressed in HEK cells, suggesting apoCaM may pre-associate with the NR1 C0 region at resting.

Keywords: Neurogranin; Calmodulin; IQ motif; Sodium channel; NMDA channel

INTRODUCTION

There is a limit to our life, but to knowledge there is no limit. —Chuang Tzu

1.1 Structure and Function of the N-Methyl-D-Aspartic Acid (NMDA) Receptor Channels

1.1.1 Overview

Glutamate receptors (GluR) contribute to excitatory synaptic transmission at sites throughout the brain and spinal cord. Based on the pharmacological properties, GluR channels have been classified into three major subtypes, that is, the α-amino-3-hydroxy-5-methyliso-4-isoxazole prop ionic acid (AMPA), Kainate and N-methyl-D-aspartic (NMDA) receptor channels. Among them, the NMDA receptor is the most clearly defined subtype due to the development of highly selective agonist NMDA (WATKINS and HASSID, 1962) and antagonist D-2-amino-5-phosphonovalerate (APV) (Davies et al., 1981). Studies with these agonist and antagonist revealed unique properties and important physiological roles of the NMDA receptor channel.

The NMDA receptors have unusual permeability properties that set them conceptually apart from the other fast ligand-gated channels. Their primary role may not be to generate electrical signals, although they do so. Instead they seem specialized for a combination of coincidence detection and transduction by elevating intracellular free [Ca^{2+}]. They have three special features. First, the NMDA receptor

channel is 5 to 10 times more permeable to Ca^{2+} ions than to Na^{+} or K^{+} (Mayer and Westbrook, 1987). Second, the channel burst time is long and the glutamate sensitivity is high compared with the rapidly desensitizing type of non-NMDA receptor channels. Finally, and surprisingly, NMDA receptors have a voltage dependence. In normal bath solution, they conduct poorly at a resting potential of -80 mV despite the presence of agonist, but when the cell is depolarized to -50 mV and glutamate is present, their conductance increases (Nowak et al., 1984). This is not a voltage-dependent activation in the sense of voltage-gated channels, for the NMDA receptor is fundamentally a ligand-gated channel. Actually, depolarization relieves a voltage-dependent block of the pore by a common extracellular ion, Mg^{2+}. Removing the physiological Mg^{2+} ion from the extracellular solution can almost eliminate the voltage dependence. In addition to requiring glutamate as an agonist, NMDA receptors also require either glycine or D-serine in the bath as co-agonists to be responsive (Johnson and Ascher, 1987b).

NMDA receptors have attracted a lot of interests in neuroscience because their functional properties suit them for participation in learning. Their voltage sensitivity enables them to serve as molecular-coincidence detectors. When glutamate is released at a synapse on a cell resting at -80 mV, the NMDA receptor pores remain blocked by Mg^{2+} and hence do nothing. But if the cell is already depolarized, the channels will open for tens of milliseconds and pass a stream of Ca^{2+} into the postsynaptic neuron. Thus they detect the coincidence of postsynaptic depolarization and presynaptic glutamates released at the synapse, and inject the postsynaptic cell with a

second-messenger ion, Ca^{2+}, that can initiate alterations of the synapse. Exactly this sequence of events underlies the induction of long term potentiation (LTP) in the CA1 region of the hippocampus, a synaptic potentiation that can be induced with a few seconds of stimulation and that can last for days (Bliss and Lomo, 1973). Furthermore, it is becoming clear that some of the most important functions of the nervous system, such as synaptic plasticity and synapse formation, critically depend on the behavior of NMDA receptor channels and that neurological damages caused by a variety of pathological states can result from exaggerated activation of NMDA receptor channels (Choi, 1988;Olney, 1990)

1.1.2 Molecular Diversity and Nomenclature of NMDA Receptors

The elucidation of the diversity of the NMDA receptor channel was one of the most important findings obtained from molecular studies (Fig. 1) (Yamazaki et al., 1992a;Moriyoshi et al., 1991b;Monyer et al., 1992a;Meguro et al., 1992a;Kutsuwada et al., 1992a;Ishii et al., 1993a;Ikeda et al., 1992a) The identification of the multiple subunits with distinct distribution, properties, implies that NMDA receptor channels are different in molecular and functional properties, depending on the brain regions and developmental stages (Mishina et al., 1993a;Seeburg, 1993). The five NMDA receptor channel subunits share significant amino acid sequence identity with the AMPA.

The two subunit families of the rat NMDA receptor channel were designated as the NMDARl (NRl) and NMDAR2 (NR2) subunit families (Ishii et al., 1993b),

whereas those of the mouse NMDA receptor channel were named the GluRε and GluRζ subunit families because they are the fifth and sixth members of the GluR channel subunit families (Ikeda et al., 1992b;Kutsuwada et al., 1992b;Meguro et al., 1992b;Yamazaki et al., 1992b).

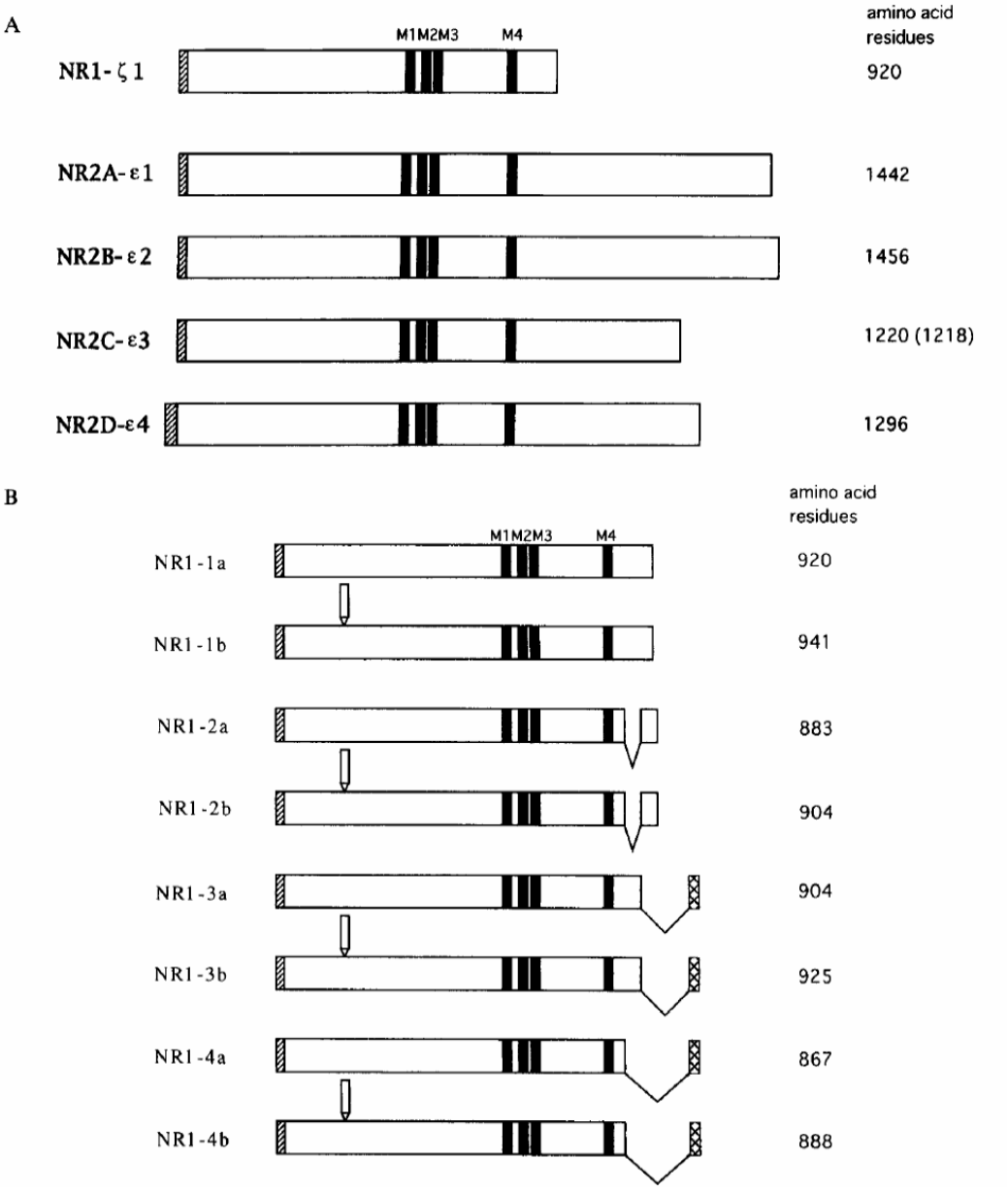

Fig. 1. Schematic representations of the NMDA receptor channel subunits. Putative signal peptides and four internal hydrophobic segments are indicated by hatched and filled boxes, respectively. Numbers of the amino acid residues of the proposed mature subunits are given; that of the rat subunit, if different from that of the mouse counterpart, is indicated in the parenthesis. (A) Five subunits. (B) Eight splice variants of the NRl-I 1 subunit. Variable sequences in the amino-and carboxyl-terminal regions are shown by open boxes above and cross-hatched boxes, respectively. (Modified from (Hollmann et al., 1993) and (Sugihara et al., 1992).

Analysis of cDNA clones suggests the presence of eight alternative splice variants of the NRl-ζ1 subunit, which are differently named by several groups [Fig. l(B)] (Anantharam et al., 1992); (Durand et al., 1992); Hollmann et al., 1993; (Nakanishi et al., 1992); Sugihara et al., 1992; Yamazaki et al., 1992). The relative abundance of the variants estimated by the number of cloned cDNAs are -67, -15 and -18% for NRl-la, variants with an amino-terminal insertion (lb, 2b, 3b and 4b), and those with carboxyl-terminal deletions (2a, 3a and 4a), respectively (Sugihara et al., 1992). No variants have been reported for the NR2A, NR2B and NR2C subunits, while the NR2D subunit exists in two forms, the NR2Dl and NR2D2 (Ishii et al., 1993).

The NRl subunit forms homomeric channels responsive to L-glutamate plus glycine and to NMDA plus glycine when expressed in Xenopus oocytes (Moriyoshi et al., 1991a); Yamazaki et al., 1992), although the current responses are very small. Pharmacological characteristics of the NRl subunit are in good agreement with those of the NMDA receptor channel.

Highly active NMDA receptor channels, however, are produced only when the NRl subunit is expressed together with one of the four NR2 subunits (Ikeda et al., 1992; Ishii et al., 1993; Kutsuwada et al., 1992; Meguro et al., 1992; (Monyer et al., 1992b). The responses of the NR2/NRl heteromeric channels to L-glutamate plus glycine were suppressed by NMDA receptor channel-selective antagonists, such as APV, 7-chlorokynurenate (7CK) (Ikeda et al., 1992; Ishii et al., 1993; Kutsuwada et al.,1992; Meguro et al., 1992; Monyer et al., 1992). The heteromeric channels exhibited clear inward currents in Na^+-and K^+-free Ringer's solution containing 20

mM Ca^{2+}, indicating their high permeability to Ca'+. These results suggest the heteromeric nature of the NMDA receptor channel. In accord with this, most brain regions express both the NR2 and NRl subunit mRNAs and no NMDA receptor channel activities have been reported for mature cerebellar Purkinje cells which express the NRl subunit but none of the NR2 subunits (Brose, 1993;Brose et al., 1993;Monyer et al., 1994;Perkel et al., 1990;Quinlan and Davies, 1985;Watanabe et al., 1992;Watanabe et al., 1994a). Heteromeric assembly of the NMDA receptor channel subunits is also suggested from the biochemical and immunological studies (Sheng et al., 1994a;Tingley et al., 1993). Anti-NRl subunit antibodies immunoprecipitated not only a -120 kDa protein but also significant amounts of the NR2A and NR2B subunits in the rat cerebral cortex (Sheng et al., 1994b). In addition, anti-NR2A subunit antibodies efficiently immunoprecipitated the NR2B subunit, and conversely, anti-NR2B subunit antibodies immunoprecipitated the NR2A subunit. These results indicate at least a portion of the NR2A and NR2B subunits are present in the same complex *in vivo*.

1.1.3 Structure

The NMDA receptor channel subunits have a putative amino-terminal signal peptide and four hydrophobic segments (Ml-M4) in the middle of the molecules. The proposed mature NR1, NR2A, NR2B, NR2C, and NR2D subunits are composed of 920, 1445, 1456, 1220 (or 1218) and 1296 amino acids, respectively, and have molecular masses of 103, 163, 163, 134 (or 133), and 141 kDa, respectively (Fig. 1)

(Ikeda et al., 1992; Ishii et al., 1993; Kutsuwada et al., 1992; Meguro et al., 1992; Monyer et al., 1992; Moriyoshi et al., 1991; Yamazaki et al., 1992). Antibodies against the NRl, NR2A, NR2B and NR2C subunits recognize -120, -170, -180 and -145 kDa proteins, respectively (Brose et al., 1993; (Chazot et al., 1992;Chazot et al., 1994;Sakimura et al., 1995;Sheng et al., 1994c)； Tingley et al., 1993). The difference between the observed and predicted values may be accounted for by glycosylation.

Overall amino acid sequence identity among NMDA receptor channel subunits is as high as -40% to -50% within the NR2 subfamily, but is as low as -18% between the NR2 and the NRl subfamilies. Amino acid sequence identity of the NMDA receptor channel subunits with other GluR channel subunits is 12-18% (Mishina et al., 1993b). The NR2-t subunits have notably larger carboxyl-terminal region than the other GluR channel subunits. The carboxyl-terminal regions of the NR2A and NR2B subunits are very long and are similar in size (627 and 644 amino acids, respectively). Although the amino acid sequence of the carboxyl-terminal region is diverse among the NR2 subunits, there is weak but clear identity (30%) between the NR2A and NR2B subunits. The carboxyl-terminal region is highly diverse between the NRl and NR2 subfamilies.

The NMDA receptor channel subunits have four hydrophobic segments (Ml-M4) in the middle of the molecules (Fig. 2). These structural characteristics seem to be common for neurotransmitter-gated ion channels, such as the nicotinic acetylcholine receptor (nAChR) channel (Noda et al., 1983), and the glycine receptor (GlyR) channel (Grenningloh et al., 1987). However, the initial four transmembrane segment

model for the NMDA receptor channel subunit (Mishina et al., 1993) may not be correct.

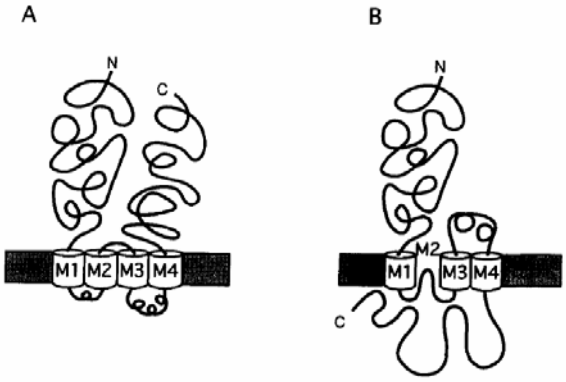

Fig. 2. NMDA channel transmembrane topology models. (A) Four transmembrane segment model. (B) Three transmembrane segment model.

Phosphopeptide map analysis suggests that the carboxyl-terminal region of the NRl subunit is phosphorylated in vivo (Tingley et al., 1993). Furthermore, the carboxyl-terminal region of the NR2 subunit is responsible for the activation of the NR1/NR2 channel by the treatment of a PKC activator, 12-U-tetradecanoyl-phorbol 13-acetate (TPA) (Mori et al., 1993). Thus, it is likely that the carboxyl-terminal region of the NRl and NR2 subunits resides on the cytoplasmic side, in contrast to the extracellular assignment based on the four transmembrane segment model. Furthermore, mutational analyses of the glycine-binding and redox modulation sites of the NRl subunit suggest the possible extracellular localization of the region between segments M3 and M4 (Kuryatov et al., 1994;Sullivan et al., 1994). These observations may be explained by a three transmembrane segment model, in which putative channel-lining segment M2 loops into the membrane without traversing it (Fig. 2).

All subunits of the NMDA receptor channel possess asparagine in segment M2 (at the position corresponding to glutamine or arginine that determine the Ca^{2+} permeability of the AMPA-selective GluR channel. Replacement by glutamine of the asparagine in segment M2 of the NR2B and NRl subunits strongly reduces the sensitivity to Mg^{2+} block of the heteromeric NMDA receptor channel. Since there is strong evidence that Mg^{2+} produces a voltage-dependent block of the channel by binding a site deep within the ionophore (Ascher and Nowak, 1988), these results are consistent with the view that segment M2 constitutes the ion channel pore of the NMDA receptor channel. As described above, segment M2 may loop into the plasma membrane from the intracellular side without actually traversing it, as proposed for the channel forming pore of the voltage-dependent ion channels (Wo and Oswald, 1995). The mutation in the NRl subunit decreases the Ca2+ permeability of the heteromeric channels whereas that in the NR2A or NR2C subunit exerts little effect (Burnashev et al., 1992).

1.1.4 Functional Diversity

Distributions of the NMDA receptor channel subunit mRNAs in the adult rodent brain were examined by in situ hybridization analyses (Akazawa et al., 1994; Ishii et al., 1993; Kutsuwada et al., 1992; Meguro et al., 1992; Monyer et al., 1992,1994; Moriyoshi et al., 1991; (Watanabe et al., 1994b;Watanabe et al., 1993). The NRl subunit mRNA is distributed ubiquitously in the brain. In contrast, the four NR2 subunit mRNAs show characteristic distributions in the brain. The NR2A subunit

mRNA is distributed widely in the brain, but the level of expression is higher in the cerebral cortex, the hippocampal formation and cerebellar granule cells. In contrast, the NR2B subunit mRNA is expressed selectively in the forebrain. High levels of expression are observed in the cerebral cortex, the hippocampal formation, the septum, the caudate-putamen, the olfactory bulb, and the thalamus. The NR2C subunit mRNA is found predominantly in the cerebellum. Strong expression is observed in the granule cell layer of the cerebellum, while weak expression is detected in the olfactory bulb and the thalamus. Low levels of the NR2D subunit mRNA are found in the thalamus, the brainstem and the olfactory bulb. Differential distributions of the NRl subunit splice variant mRNAs were suggested in the rat basal ganglia (Laurie and Seeburg, 1994;Standaert et al., 1994).

NMDA receptor channels are characterized by slow gating (Lester and Jahr, 1992). The offset decay time constant of the NRl/NR2A channel is ~120 msec and that of the NRl/NR2B or NRl/NR2C channel is ~400 msec. On the other hand, the NRI/NR2D channel shows a very long offset decay time constant (-5000 msec) (Monyer et al., 1994)

NMDA-mediated excitatory postsynaptic currents (EPSCs) in neurons of the visual cortex layer IV last longer in young rats, and their duration become progressively shorter (Carmignoto and Vicini, 1992). Furthermore, the duration of NMDA receptor channel mediated EPSCs in the superior colliculas is several times longer at early developmental stages than that of older animals (Hestrin, 1992). It remains to be established whether these changes during development are related to a

switch of the subunit composition of the NMDA receptor channel.

NMDA receptors are activated by glutamate, and structurally related acidic amino acids such as NMDA and aspartate but not AMPA or kainate, provided that the co-agonist glycine is present simultaneously (Johnson and Ascher, 1987a). Analysis of the action of conformationally restricted analogues of glutamate suggests that glutamate binds to NMDA receptors in a folded conformation, different from that required for activation of AMPA and kainate receptors. There is now substantial evidence indicating interactions between the binding sites for glutamate and glycine, which are best explained by allosteric mechanisms. From analysis of the kinetics of NMDA receptor activation by glutamate and glycine, it is generally agreed that two molecules of glutamate, and two molecules of glycine, must bind to native NMDA receptors on hippocampal neurons to activate ion channel gating (Benveniste et al., 1990). Competitive antagonists acting at the binding sites for the co-agonists glutamate and glycine have a distinct pharmacology and are thus likely to act at separate locations on the NMDA receptor channel complex. However, the sites for glutamate and glycine appear to be allosterically coupled, such that binding of glutamate decreases NMDA receptor affinity for glycine approximately sevenfold (Benveniste et al, 1990). Such allosteric regulation of NMDA receptor activity is of potential physiological significance, given the observation that glycine is thought to be present continuously within the extracellular space, while glutamate is released transiently from nerve terminals. The widespread expression of mRNA for a glycine transporter throughout the CNS, with a distribution overlapping that for NMDAR1,

suggests that the extracellular concentration of glycine is tightly regulated. Because both glutamate and glycine must remain bound to an NMDA receptor channel complex to activate ion channel gating, the negative allosteric coupling between binding of glutamate and binding of glycine produces responses which appear to inactivate (Mayer et al., 1989). Such responses have been observed both with whole cell recording (Benveniste et al, 1990) and also in outside-out patches (Parsons et al., 1993), but are complicated by the development of other forms of NMDA receptor inactivation.

Three forms of NMDA receptor inactivation are currently recognized. Examples are illustrated in Fig. 3 and include Ca^{2+}- and glycine independent inactivation, which occurs following binding of glutamate and which is likely to be comparable to the inactivation recorded at other types of ligand-gated ion channel (Sather et al., 1990); calcium dependent inactivation mediated by a rise in the activity of intracellular Ca^{2+}, resulting from ion flux through NMDA receptor channels; and so-called glycine-sensitive inactivation (Mayer et al., 1989). The latter mechanism underlies the fade in response to NMDA that occurs when the receptor is first equilibrated with a low concentration of glycine (1μM or lower), before the application by rapid perfusion of glutamate or NMDA, and is not true inactivation but due to dissociation of glycine from its binding site triggered by the interaction of increase in the concentration of glycine prevents this fade in response to glutamate because, at a sufficiently high concentration of glycine, ~10μM, the probability of occupancy of the glycine binding site remains high despite the drop in affinity of the NMDA receptor

for glycine that occurs on binding of glutamate.

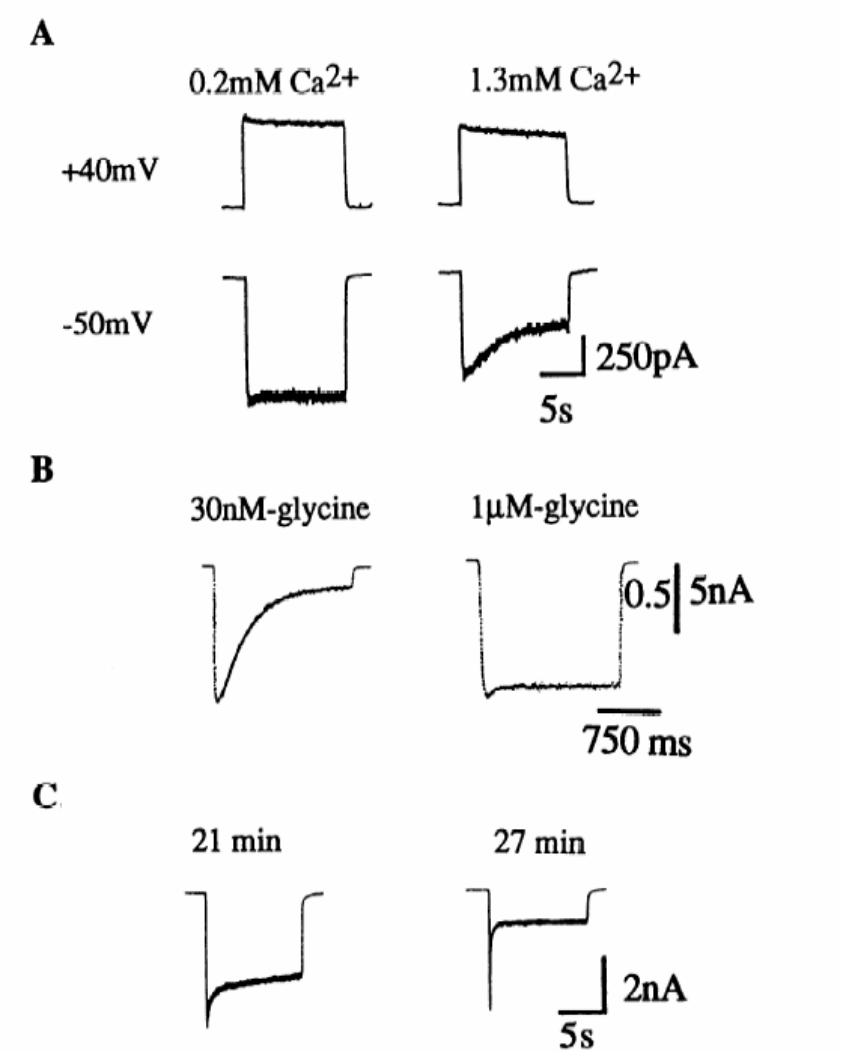

Fig. 3. Multiple forms of NMDA receptor desensitization. A: Ca2+-dependent desensitization due to Ca2+ entry through NMDA receptor channels at -50 but not +40 mV. (From (Legendre et al., 1993) B: "glycine-sensitive" desensitization recorded with 0.2 mM extracellular Ca^{2+} in presence of 30 nM but not 1 μM glycine. (From Mayer et al., 1989). C: Ca^{2+}- and glycine-independent desensitization that occurs following prolonged whole cell recording. (From Mayer et al.， 1989)

1.1.4 Physiological Properties

Tetanic stimulation-induced LTP of synaptic transmission in the hippocampus has been extensively studied as a model of activity-dependent change in synaptic efficacy, which is thought to provide the physiological basis for information storage in the brain (Bliss and Collingridge, 1993). APV administration reversibly prevented the induction of LTP in the CA1 region of the hippocampus (Collingridge et al., 1983)). During tetanic stimulation, there is a greater and longer-lasting depolarization, which alleviates the Mg^{2+} block of NMDA channels. The activated NMDA receptor channels are permeable to Ca^{2+} (Ascher and Nowak, 1986;(MacDermott et al., 1986) and Ca^{2+} enters the cell via NMDA receptor channel and triggers the processes leading to a sequence of events that culminate in enhanced synaptic efficacy. Thus, it is the NMDA receptor channel that acts as the associative switch for the induction of LTP, turning on only when postsynaptic depolarization is paired temporally with the synaptic release of glutamate. Recent studies suggest that the NMDA receptor channel plays a key role in divert forms of synaptic plasticity including LTD (Bliss and Collingridge, 1993; (Malenka and Nicoll, 1993). The relationship between the NMDA receptor channel-dependent synaptic plasticity and learning has been examined by two independent approaches. Morris and his colleagues demonstrated that chronic intraventricular infusion of APV impaired both hippocampal LTP and spatial learning in rat (Davis et al., 1992;Morris et al., 1986). Mutant mice defective in the ε1 subunit of the NMDA receptor channel produced by gene targeting showed the significant reduction of the NMDA receptor channel current and LTP at the hippocampal CA1

synapse (Sakimura et al., 1995). The mice also showed moderate deficiency in spatial learning. These results support the notion that the NMDA receptor channel-dependent synaptic plasticity is the cellular basis of certain forms of learning.

The N-methyl-D-aspartate (NMDA) class of glutamate receptor/channel plays critical roles in such fundamental phenomena as synaptic transmission, synaptic plasticity, synapse formation, and excitotoxic cell death in the mammalian central nervous system. As mentioned, a key property of the NMDA receptor ion channel that contributes to these multiple roles is that it exhibits a high permeability to calcium. Work by Mark Mayer and Gary Westbrook (Mayer and Westbrook, 1985), and subsequently by many other laboratories (Zhang et al., 1998;Krupp et al., 1999), has demonstrated that receptor-mediated calcium influx leads to rapid calcium-dependent inactivation of NMDA receptors. More recent evidence implicates calmodulin in this calcium-dependent inactivation process. As mentioned above, NMDA receptor channels are hetero-oligomeric complexes containing members of the homologous NR1 and NR2 subunit families. Richard Huganir and his colleagues found that calmodulin binds to a portion of the carboxy-terminal domain of the NR1 subunit, and that this interaction reduces the open probability of NMDA receptor channels in a manner that can account for calcium-dependent inactivation (Ehlers et al., 1996). Inactivation in neurons may actually be more complicated and more interesting, involving yet another NR1 binding partner, the actin-binding protein α-actinin that competes with calmodulin for binding to NR1 (Wyszynski et al., 1997). Experiments from the Huganir and Westbrook laboratories suggest that inactivation may occur

when calcium-bound calmodulin competitively displaces α-actinin from the NR1 subunit, thereby releasing the receptor/channel from its attachment to the actin cytoskeleton (Zhang et al., 1998; Krupp et al., 1999). Calcium may also bind directly to α-actinin and thereby reduce its affinity for NR1, independent of the displacement by calcium/calmodulin (Krupp et al., 1999).

1.2 Structure and Function of the Voltage-gated Sodium Receptor Channels

1.2.1 Overview

Voltage-gated sodium channels play an essential role in the initiation and propagation of action potentials in neurons and other electrically excitable cells such as myocytes andendocrine cells. When the cell membrane is depolarized by a few millivolts, sodium channels activate and inactivate within milliseconds. Influx of sodium ions through the integral membrane proteins comprising the channel depolarizes the membrane further and initiates the rising phase of the action potential. The voltage-gated sodium channel is a large, multimeric complex, composed of an α subunit and one or more smaller β subunits (Catterall, 2000). The ion-conducting aqueous pore is contained entirely within the α subunit, and the essential elements of sodium such as channel function, channel opening, ion selectivity and rapid inactivation can be demonstrated when α subunits are expressed alone in heterologous cells. Co-expression of the β subunit is required for full reconstitution of the properties of native sodium channels, as these auxiliary subunits modify the kinetics and voltage-dependence of the gating (that is, opening and closing) of the channel.

Although different sodium channels have broadly similar functional characteristics, small differences in properties do distinguish different isoforms and contribute to their specialized functional roles in mammalian physiology and pharmacology.

1.2.2 Sodium channel subunits and structure

Sodium-channel proteins in the mammalian brain are composed of a complex of a 260 kDa α subunit in association with one or more auxiliary β subunits (β1, β2 and/or β3) of 33-36 kDa (Catterall, 2000). Nine α subunits (Nav1.1-Nav1.9) have been functionally characterized and a tenth relate isoform (Nax) may also function as a Na^+ channel. The primary sequence predicts that the sodium channel α subunit folds into four domains (I-IV), which are similar to one another and contain six α-helical transmembrane segments (S1-S6). In each of the domains, the voltage sensor is located in the S4 segments, which contain positively charged amino-acid residues in every third position. A reentrant loop between helices S5 and S6 is embedded into the transmembrane region of the channel to form the narrow, ion-selective filter at the extracellular end of the pore. The wider intracellular end of the pore is formed by the four S6 segments. Small extracellular loops connect the transmembrane segments, with the largest ones connecting the S5 or S6 segments to the membrane re-entrant loop. Larger intracellular loops link the four homologous domains. Large amino-terminal and carboxy-terminal tail domains also contribute to the internal face of the sodium channel. This view of sodium channel architecture has been largely confirmed by biochemical, electrophysiological, and structural experiments. A

complete three-dimensional structure of the sodium channel is not yet available; however, limited but interesting structural information on the sodium channel is beginning to emerge. Direct structural determination at 19 Å resolution by cryo-electron microscopy and image reconstruction techniques (Sato et al., 2001) show sodium channels as having a bell-like shape (when viewed from the side), with a four-fold symmetry of transmembrane masses and large intracellular and extracellular masses through which several inlets and outlets allow aqueous access (Figure 4b). Unexpectedly, this image of sodium channels predicts a central pore that does not directly connect the intracellular and extracellular spaces but instead splits into four branches. Moreover, it suggests that there are four peripherally located transmembrane pores of unknown function, possibly acting as gating pores for voltage-sensor movement. The solution structure of the inactivation gate on the intracellular loop between domains III and IV has been determined by nuclear magnetic resonance (NMR). This analysis predicts a rigid α-helical structure, preceded by two turns that position a key hydrophobic sequence motif (the IFM motif, Ile-Phe-Met) such that it can interact with and block the inner mouth of the pore (Figure 5). The global fold of the sodium-channel pore region is predicted to be largely similar to that of potassium channels, whose structure has been solved by X-ray crystallography (Doyle et al., 1998). In this hypothetical structural view, the S5 and S6 helices of each sodium-channel domain are arrayed in four-fold symmetry around the aqueous ion-conduction pathway and the pore is lined mostly by S6 segments and the re-entrant loops that form the ion-selectivity filter.

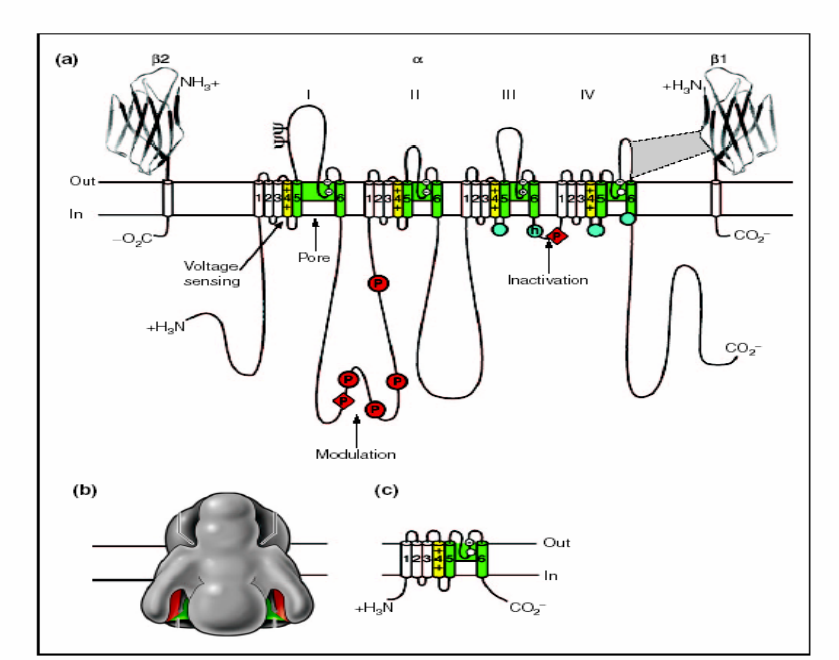

Fig. 4.

Structure of voltage-gated sodium channels. **(a)** Schematic representation of the sodium-channel subunits. The α subunit of the Nav1.2 channel is illustrated together with the β1 and β2 subunits; the extracellular domains of the β subunits are shown as immunoglobulin-like folds, which interact with the loops in the α subunits as shown. Roman numerals indicate the domains of the α subunit; segments 5 and 6 (shown in green) are the pore lining segments and the S4 helices (yellow) make up the voltage sensors. Blue circles in the intracellular loops of domains III and IV indicate the inactivation gate IFM motif and its receptor (h, inactivation gate); P, phosphorylation sites (in red circles, sites for protein kinase A; in red diamonds, sites for protein kinase C); ψ, probable *N*-linked glycosylation site. The circles in the re-entrant loops in each domain represent the amino acids that form the ion selectivity filter (the outer rings have the sequence EEDD and inner rings DEKA). **(b)** The three-dimensional structure of the Nav channel α-subunit at 20 Å resolution, compiled from electron micrograph reconstructions. **(c)** Schematic representation of NaChBac, the bacterial voltage-gated sodium channel. Adapted from (Sato et al., 2001).

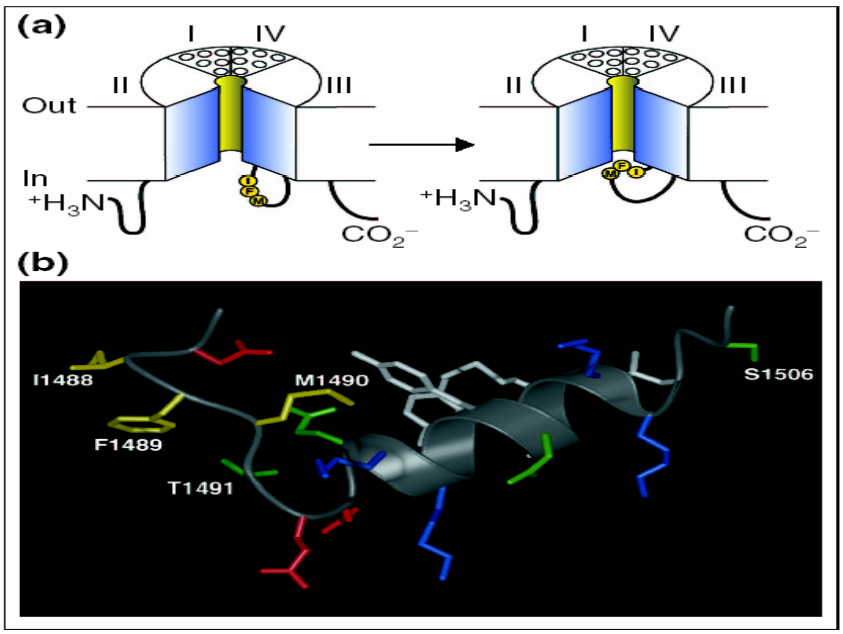

Fig. 5.
Mechanism of inactivation of sodium channels. **(a)** The hinged-lid mechanism. The intracellular loop connecting domains III and IV of the sodium channel is depicted as forming a hinged lid with the critical phenylalanine (F1489) within the IFM motif shown occluding the mouth of the pore during the inactivation process. The circles represent the transmembrane helices. **(b)** Three-dimensional structure of the central segment of the inactivation gate, as determined by multidimensional NMR. Side chains of the critical IFM motif residues (I1488, F1489 and M1490) are shown in yellow, and those of T1491, which is important for inactivation, and S1506, which is a protein-kinase-C-dependent phosphorylation site, are also indicated. Adapted from (Rohl et al., 1999).

1.2.3 Molecular basis of function

Classical work by Hodgkin and Huxley (HODGKIN and HUXLEY, 1952b) defined the three key features of sodium channels: voltage-dependent activation, rapid inactivation, and selective ion conductance. Building on this foundation, more recent structure-function studies using molecular, biochemical and electrophysiological techniques have provided us with a good understanding of the molecular basis of sodium-channel function. Critical to this were the neurotoxins tetrodotoxin and saxitoxin, whose pore-blocking properties were exploited to purify the

sodium-channel proteins and to reveal the amino-acid residues involved in the outer pore and in the selectivity filter. The outer pore is formed by the re-entrant loops between transmembrane segments S5 and S6 of each domain. Two important amino acids in analogous positions in all four domains are thought to form the negatively charged outer and inner rings that serve as a receptor site for pore-blockers and the selectivity filter (Figure 4a). Mutations of these residues have significant effects on binding of tetrodotoxin and saxitoxin (Noda et al., 1989), and also have marked effects on the selectivity of permeation of organic and inorganic monovalent cations through the sodium channel (Schlief et al., 1996). The most convincing evidence comes from a study by Heinemann et al. (Heinemann et al., 1992), who produced a calcium-selective sodium channel by mutating the inner ring residues (DEKA in the single-letter amino-acid code) to their counterparts in calcium channels (EEEE). As is the case for other voltage-gated ion channels, the voltage-dependence of activation of sodium channels derives from the outward movement of charged residues as a consequence of an altered electric field across the membrane (HODGKIN and HUXLEY, 1952a). The S4 segments of each homologous domain serve as the voltage sensors for activation. They are composed of repeated motifs of one positively charged residue followed by two hydrophobic residues, potentially creating a helical arrangement of positive charges through the membrane.

Upon depolarization, the outward movement of the S4 helices and their concurrent rotation initiates a conformational change that opens the sodium-channel pore. This ‘sliding helix’ (Catterall, 1986) or ‘helical screw’ (Guy and

Seetharamulu, 1986) model is supported by strong evidence. For example, neutralization of the key positively charged residues in S4 markedly reduces the voltage-dependence of gating (Stuhmer et al., 1989). The outward gating movement of the S4 segments has also been detected directly by the fact that, when some residues in these helices are substituted with cysteines, extracellular sulfhydryl reagents react with them only after channel activation (Cha et al., 1999;Yang et al., 1996;Yang and Horn, 1995). Inactivation of the sodium channel is a critical process that occurs within milliseconds of channel opening. In the generally accepted model of this process, the highly conserved intracellular loop that connects domains III and IV serves as an inactivation gate, much like a hinged lid, that binds to the intracellular pore of the channel to inactivate it (Figure 5a). Intracellular perfusion of proteases (Armstrong, 1981) or intracellular application of antibodies that recognize this loop, but not antibodies to other intracellular structures (Vassilev et al., 1989), prevents fast inactivation. The ‘latch’ of the inactivation gate is formed by three key hydrophobic residues (IFM; Figure 5), and peptides containing this motif can restore inactivation to sodium channels that have a mutated inactivation gate (Eaholtz et al., 1994). Mutations of the key phenylalanine residue (Phe1489) to various hydrophilic residues impair inactivation to varying degrees. Furthermore, if it is replaced with a cysteine residue, covalent modification of the cysteine is prevented when the inactivation gate is closed (Kellenberger et al., 1996). Structural determination and NMR analysis of the core portion of the inactivation gate reveal a rigid α-helical structure flanked by the IFM motif (Figure 5b). In this structure, the side-chain of Phe1489 points away

from the core of the peptide on the same face as a nearby threonine (Thr1491), another critical residue for inactivation (Kellenberger et al., 1996). In contrast to the short IFM motif that forms the inactivation gate, the receptor for the inactivation gate on the body of the channel may be composed of multiple hydrophobic residues near the intracellular mouth of the pore. Scanning mutagenesis experiments implicate hydrophobic residues in intracellular loops S4-S5 of domains III and IV, as well as the intracellular end of the S6 transmembrane segments of these domains, as components of the inactivation gate receptor. The exciting discovery of a bacterial sodium channel (NaChBac; Figure 4c), consisting of a single domain of six transmembrane α-helical segments (Ren et al., 2001), potentially provides new tools for the study of the sodium channel structure-function relationships. The NaChBac channel apparently forms a homotetramer that is a functional voltage-gated sodium channel. It has a 100-fold slower rate of inactivation than the Nav channels (because it has no equivalent of the inactivation gate). Furthermore, its sodium selectivity filter appears to be symmetric, formed by four glutamate residues in key positions in all four pore loops, resembling that of the Ca^{2+} channel. This bacterial sodium channel will provide a simpler framework than the mammalian channels for mutagenesis experiments to test hypotheses regarding the structure and function of voltage gated sodium channels. In addition, the small size of the channel may make it easier to obtain crystal-structure information, as has been the case for the pore region of the bacterial potassium channel (KcsA).

1.2.4 Localization and modulation

In addition to the differences in cellular and tissue expression, mammalian sodium channels also have differential expression profiles during development and different subcellular localizations, consistent with a distinct role for each channel in mammalian physiology. In rodents, Nav1.3 is highly expressed in fetal nervous tissues, whereas Nav1.1, Nav1.2, and Nav1.6 are abundant in the adult central nervous system. Generally, Nav1.1 and Nav1.3 are localized to the soma of the neuron, where they may control neuronal excitability through integration of synaptic impulses to set the threshold for action potential initiation and propagation to the dendritic and axonal compartments. Evidence from immunocytochemical experiments indicates that Nav1.2 is expressed in unmyelinated axons, where it conducts the action potential (Westenbroek et al., 1989). During development, Nav1.6 has been shown to replace Nav1.2 in maturing nodes of Ranvier, the gaps in the myelin sheaths of myelinated axons where action potential conduction takes place (Boiko et al., 2001;Kaplan et al., 2001). Nav1.1 and Nav1.6 are also significantly expressed in the peripheral nervous system (PNS), but the sodium channels that are the most abundantly expressed in the PNS are the three isoforms that have been cloned from sympathetic and dorsal root ganglion neurons, namely Nav1.7, Nav1.8 and Nav1.9. Of these, Nav1.7 is broadly expressed in the PNS and appears to be localized to axons, where it may function in initiating and conducting the action potential (Toledo-Aral et al., 1997). More restricted expression patterns are observed for Nav1.8 and Nav1.9; these channels are differentially expressed in small sensory neurons of the dorsal root

and trigeminal ganglia, where they have a key role in the perception of pain (Black et al., 1999). Finally, Nav1.4 and Nav1.5 are muscle sodium channels that control the excitability of the skeletal and cardiac myocytes, respectively. Nav1.5 is transiently expressed in developing skeletal muscle but is replaced by Nav1.4 in the adult.

Sodium-channel function is known to be regulated in neurons in response to physiological signals [reviewed in (Cantrell and Catterall, 2001a)]. The neurotransmitter dopamine has been shown to modify the firing properties and the input-output properties of medium spiny neurons of the ventral and dorsal striatum, acting through D1-like dopamine receptors and activation of the cAMP pathway to reduce sodium currents and the generation of action potentials. Biochemical studies have shown that purified sodium channels are phosphorylated by the cAMP-dependent protein kinase A at multiple sites in the intracellular loop between domains I and II (Cantrell and Catterall, 2001b). In another example of modulation of sodium channels by neural signals, activation of muscarinic acetylcholine receptors by the neurotransmitter acetylcholine inhibits the intrinsic bursts of firing activity of hippocampal CA1 neurons. This effect is mediated in part by protein-kinase-C-dependent phosphorylation of a highly conserved residue (Ser1506 of Nav1.2) in the inactivation gate, which slows sodium-channel inactivation and reduces the peak sodium currents in the neurons. Additional phosphorylation of sites in intracellular loop I-II also influences regulation of sodium channels by protein kinase C (Cantrell and Catterall, 2001c). Moreover, activation of tyrosine kinase pathways has also been implicated in sodium-channel modulation (Hilborn et al.,

1998), as has converse regulation by a receptor tyrosine phosphatase, RPTPβ (Ratcliffe et al., 2000). Additional modulation of sodium channels by other second messenger systems, including the G-protein subunits $G_{\beta\gamma}$ (Ma et al., 1997) and calcium/calmodulin (Tan et al., 2002), is also observed in transfected mammalian cells.

1.3 Characteristics of Neurogranin (Ng)

1.3.1 Overview

Neurogranin (Ng), also known as RC3 and p17, is a neuron-specific protein that is selectively expressed high levels in neuronal cell bodies and dendrites of the cerebral cortex, hippocampus and striatum. It was first identified as a brain-specific protein kinase C (PKC) substrate in bovine, and also as a rodent cortex-enriched mRNA by screening a rat brain cDNA library (Watson et al., 1990;Baudier et al., 1989;Gerendasy and Sutcliffe, 1997).

Ng resembles closely a presynaptic PKC substrate neuromodulin (Nm, also known as Gap-43, F1 or B-50). Ng and Nm share high sequence homology within 20 amino acids designated as the IQ motif, which contains a binding domain for calmodulin (CaM) and a PKC phosphorylation site. The interaction between CaM and the IQ motif of Ng and Nm has been characterized extensively. CaM binds to both proteins in a Ca^{2+}-sensitive manner, namely, Ng or Nm forms a complex with CaM in the absence of Ca^{2+} (Baudier et al., 1991;Huang et al., 1993a;Gerendasy et al., 1995). PKC phosphorylation within the IQ motif inhibits CaM binding, and conversely, CaM

binding inhibits PKC phosphorylation at serine within the IQ domain. These observations led to the general hypothesis that Ng and Nm may bind CaM at specific sites in neurons and that PKC phosphorylation or changes in Ca^{2+} may result in the increase of free CaM level for the activation of many Ca^{2+}/CaM dependent enzymes in the neurons.

Rat and mouse brain Ng contains four cysteine residues that are readily oxidized by physiological oxidants *in vitro*, such as nitric oxide, superoxide and hydrogen peroxide, as well as by neurotransmitter N-Methyl-D-Aspartic Acid (NMDA) in brain slices *in situ* (Sheu et al., 1996;Li et al., 1998). Upon oxidization, Ng preferentially forms two pairs of intermolecular disulfide bonds. The fine-tuned control of the release of CaM, and maintenance of intracellular levels of free Ca^{2+} and CaM, are regulated by both the phosphorylation and oxidization of Ng.

Although the physiological functions of Ng have not been defined, its biochemical properties and postsynaptic localization have implicated that Ng may play pivotal roles in long term potentiation (LTP) by releasing CaM. LTP has been extensively studied as potential synaptic mechanisms involved in information storage during learning and memory. It is now clear that LTP has many forms, which can be distinguished on the basis of their underlying signal mechanisms. One of the best forms of LTP is related to NMDA-type glutamate receptors.

1.3.2 Expression pattern

The cellular and subcellular localizations and the pattern of expression of Ng during development, in many respects, resemble those of the protein kinase C (PKC)-γ isozyme which is also a neuron-specific protein. However, the Ng gene has a more restricted neuronal expression than PKC-γ. The characteristic brain-specific and developmental stage-regulated expression of these two proteins is distinctively different from that of PKC-α and -β. These latter two PKCs are ubiquitously expressed in a variety of tissues and cell types. Like Ng, the expression of PKC-γ is progressively increased from the fetal stage up to 2-3 weeks after birth. The mechanisms that trigger the delayed expression of both PKC-γ and Ng are unknown.

1.3.3 IQ motif

Ng binds to CaM *in vivo* and is the only Ng-interacting protein isolated from brain cDNA libraries. Single amino acid mutagenesis indicated that residues within the specific domain of Ng are important for CaM binding *in vivo* (Prichard et al., 1999). This domain begins with isoleucine and glutamine, so was called IQ motif (Figure 6), which is very conservative with other CaM-binding proteins. Ng was shown to be phosphorylated in hippocampal slices incubated with ^{32}Pi and phorbol ester, suggesting Ng is an *in vivo* substrate of PKC. Tryptic digestion of the phosphorylated protein yielded a single phosphopeptide having the sequence of IQASFR, where the serine residue is the phosphorylated amino acid, and the Ser^{36} is adjacent to the CaM-binding domain (Ala^{29}-Ser^{48}) (Huang et al., 1993b).

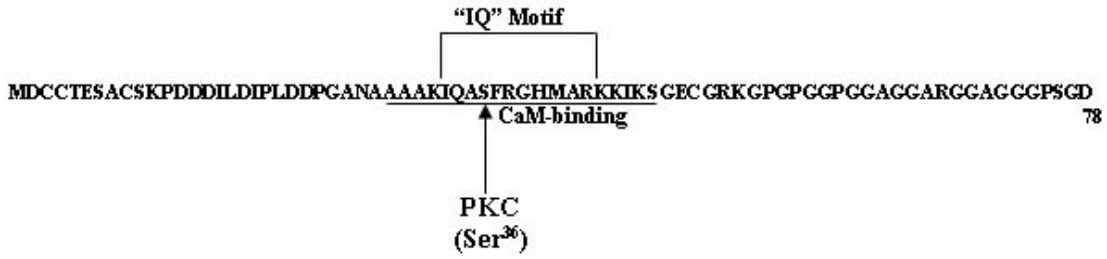

Figure 6. The "IQ" motif in Ng. The consensus sequence for the "IQ" motif is bracketed within the Ng amino acid sequence. Serine[36], the site of PKC phosphorylation, is indicated by an arrow while the CaM-binding domain is denoted by a line below the sequence.

1.3.4 The role of Ng in the regulation of intracellular calcium concentration

Ca^{2+} is a crucial regulator of many physiological processes, and a variety of stimuli produce their cellular effects by regulating the cytosolic free Ca^{2+} concentration ($[Ca^{2+}]_i$). Cytosolic Ca^{2+} is a major second messenger in virtually every cell throughout all life forms. In the nervous system, changes in $[Ca^{2+}]_i$ can play roles in many aspects of neuronal activity, ranging from rapid modulations of channel function within a millisecond timescale (Levitan, 1999), and presynaptic neurosecretion (Burgoyne and Morgan, 1995;Bennett et al., 1997) to long-term switches in gene expression (Berridge, 1998). Ironically, this much used mode of signaling in neurons can also contribute to cellular demise since uncontrolled increases in cytosolic Ca^{2+} contribute to excitotoxicity and neuronal death. In eukaryotes, Ca^{2+} from the extracellular space enters the cell through various types of Ca^{2+} channels as well as the sodium-calcium exchanger. Ca^{2+} can also be released

from internal Ca^{2+} stores through IP_3 receptor or ryanodine receptors, and it is taken up into these organelles by means of Ca^{2+} pumps. The Ca^{2+} release from intracellular store is usually transient. However a sustained increase in cytosolic Ca^{2+} is required for many processes. Therefore, Ca^{2+} influx into the cell is crucial to maintain the cytosolic Ca^{2+} level. In excitable cells, voltage-gated Ca^{2+} channels on the cell membrane are responsible for most of the Ca^{2+} influx pathway. It has been particularly well studied in neuronal cells, in which depolarization of the plasma membrane causes an influx of Ca^{2+} into the nerve terminal, initiating the secretion of neurotransmitters. Ca^{2+} enters through voltage-gated Ca^{2+} channels that open when the plasma membrane of the nerve terminal is depolarized by an invading action potential. There are at least five types of voltage-gated Ca^{2+} channels known as L-, T-, N-, P- and Q-type. All of them have been well characterized on the basis of their single-channel conductance, voltage dependence, pharmacological profile and molecular biology.

Generally, Ca^{2+} elicits two types of signaling events. First, Ca^{2+} can directly alter the activity of a number of enzymes and channels. Indeed, overactivation of proteases, such as calpains, is thought to underlie some of the deleterious properties of glutamate excitotoxicity. Second, Ca^{2+} can bind to the ubiquitous modulator, CaM, which in its Ca^{2+}-bound state can alter the properties of other proteins. Many of these proteins are themselves components of signaling cascades that have been implicated in diverse neuronal functions. For example, CaM-mediated signaling has been

implicated in LTP, gene expression, maintenance of the cytoskeleton, response to stress, axonal growth, the coordination of metabolic events, and cell death.

Ca^{2+} plays an important role in regulating a great variety of neuronal processes. Like other cells, neurons use both extracellular and intracellular sources of Ca^{2+}. The mechanisms responsible for regulating the influx of external Ca^{2+} are well established. For example, voltage-operated channels are used to trigger the release of neurotransmitter at synaptic junctions and they contribute to dendritic action potentials. In addition, neurotransmitters can induce an influx of Ca^{2+} using receptor-operated channels such as the NMDA receptors located primarily at postsynaptic sites. Recently, the store-operated influx has been found in neurons (Emptage et al., 2001). While much is known about these influx pathways, there is less information on the mechanism and role of the intracellular supply of Ca^{2+} stored within the ER of neurons. IP_3 receptors or ryanodine receptors distributed throughout the ER are responsible for releasing Ca^{2+} from this internal store. The phosphoinositide system is particularly well developed in the brain. A large number of different receptors respond by stimulating the hydrolysis of phosphatidylinositol 4, 5-bisphosphate (PIP_2) to form the second messenger diacylglycerol (DAG) and IP_3. IP_3 acts by releasing Ca^{2+} from the IP_3 receptors, which are widely distributed throughout the brain. Much of the evidence for IP_3-induced Ca^{2+} release has come from studying cultured neurons (Geiling and Schild, 1996; Irving *et al*., 1992; Linden, 1994; Seymour-Laurent and Barish, 1995).

The hypothesis that Ng functions by modulating the IP_3/DAG second messenger pathway after its phosphorylation by PKC was indirectly tested by heterologous expression in *Xenopus* oocytes. Acetycholine-evoked inward chloride currents, dependent on both IP_3 release and intracellular Ca^{2+}, were 2- to 3-fold higher in Ng-injected oocytes than in uninjected control oocytes. Ng-oocytes did not exhibit enhanced currents when preincubated with the protein kinase inhibitor or when a glycine residue was substituted for serine[36], the PKC phosphorylation site of Ng. Activation of endogenous oocyte PKC by phorbol esters generated inward Cl^- currents in Ng oocytes but not in control oocytes. The evidence suggested that PKC-phosphorylated Ng is capable of enhancing the mobilization of intracellular Ca^{2+} in *Xenopus* oocytes and may play a role in Ca^{2+} homeostasis in dendrites of forebrain neurons (Cohen *et al*., 1993).

1.3.5 Implications for LTP

The Ng might best be thought of as a component of a system designed to transform an initial signal, in the form of a Ca^{2+} flux, into one of several graded outputs. The output for a given signaling event would be a modified flux of Ca^{2+} adjusted to the concentration range necessary to trigger the required combinations of Ca^{2+}-dependent second-messenger cascades. In the neuron, the system is amenable to dynamic tuning through Ca^{2+}-dependent phosphorylation and dephosphorylation of Ng. The basal phosphorylation states of Ng set when the rate of PKC-mediated phosphorylation and calcineurin-mediated dephosphorylation are at equilibrium. Arise

in Ca^{2+} would change the rates of both enzymes, causing an adjustment in the state of Ng phosphorylation. Presumably the change would involve a net increase in phosphorylation, which would decrease [Ca^{2+}] by increasing the buffering capacity of the system and thereby maintain homeostasis. Increased phosphorylation also causes increased concentrations of free CaM, which further activates calcineurin, ensuring that Ng return to its basal phosphorylation state. By itself, Ca^{2+} cannot fully activate PKC, so one would not expect large amounts of Ng to be phosphorylated by Ca^{2+} fluxes alone. In addition to the NMDA receptor, LTP requires the activation of the metabotropic glutamate receptor and consequent production of diacylglycerol (DAG) and inositol 1,4,5-trisphosphate (IP3). DAG activates PKC provided there is sufficient Ca^{2+}. Because influxes through the NMDA receptor are translated into higher Ca^{2+} concentrations when Ng is not phosphorylated, activation of PKC by DAG will be more effective when the phosphorylation state of Ng is low and less effective when it is high, providing another level of homeostatic regulation. When IP3 binds to the IP3 receptor, internal Ca^{2+} is mobilized, amplifying the effects of the initial influx of Ca^{2+}. The extent to which internal Ca^{2+} is mobilized depends on the Ca^{2+} concentration in the cytoplasm. The optimum Ca^{2+} concentration is approximately 300 nM Ca^{2+} (Berridge, 1993). Whether or not this optimum is achieved through an influx of external Ca^{2+} will depend on the phosphorylation state of the calpacitin. As it is phosphorylated, the optimum will become more difficult to achieve, and there will be a downward pressure on Ca^{2+} concentrations. Also, as the phosphorylation state of Ng increase, CaM becomes increasingly available to CaM-dependent enzymes and, thus,

the later stages of the LTP signaling cascade are set into motions. Unphosphorylated, the two calpacitins compete fairly effectively with CaM-dependent enzymes involved in the induction of LTP such as CaMKII (50 nM affinity) and adenylylcyclase (Meyer et al., 1992). As CaM is made available to various enzymes of the LTP signaling cascade, Ca^{2+} is more effectively buffered, leading to decreased PKC activity and IP3 receptor sensitivity. Calcineurin requires less Ca^{2+} to maintain a high level of activity when it is bound to Ca^{2+}/CaM, so its activity probably remains high even as Ca^{2+} levels decrease (Stemmer and Klee, 1994). These events bring Ng back to its basal phosphorylation state, decrease the availability of CaM, and provide a mechanism for the homeostatic regulation of all enzymes involved. Thus, in addition to adjusting Ca^{2+} fluxes to the proper levels, Ng serves to dampen the system. In its basal state, Ng amplifies the effects of Ca^{2+} influxes, making the system more sensitive. At the height of activity, it acts to bring the system back to the basal state and, in so doing; it initiates downstream events that lead to LTP.

1.4 Objectives of this study

The goal of the study was to find out, firstly, whether Ng peptides can regulate the functional properties of Sodium channel and NMDA receptor channel; secondly, what is the molecular mechanism accounting for this regulation, if any.

MATERIALS AND METHODS

2.1 Cortical neuron culturing

2.1.1 Coating

On the day before dissection, incubate the glass coverslips with 0.1mg/ml Poly-L-Ornithine (Sigma, USA) at 37^{o}C overnight. On the day of dissection, wash the coverslips with Phosphate Buffer Saline (PBS) (NUMI, Singapore) for 3 times.

2.1.2 Dissection

All dissection tools were sterilized by boiling in MilliQ water before dissection. Brains were obtained by decapitating one-day old Swiss albino mice and the cortical regions were immediately dissected. Other regions of the brains such as the hippocampus, hypothalamus and the hindbrain were carefully teased off. The cortical regions of the brain were then immediately put in 1X PBS solution containing 100 units/ml Penicillin/Streptomycin (Gibcol, USA) and 10 mM glucose. A steady stream of oxygen gas was bubbled through the medium to ensure sufficient oxygen for the brains. After the decapitation procedure, the brains were then minced and transferred to another fresh medium of composition similar to the first. The cells were then centrifuged for 5 minutes at 18^{o}C at 1000 rpm. The supernatant was discarded, and the cells were resuspended with 6 ml of 3X trypsin solution in PBS. 0.6 ml of DNAse was added to the mixture and the cells were then incubated at room temperature for 20 minutes with oxygen perfusion. 6 ml of Dulbecco's Modified Eagle Medium (DMEM, Gibcol, USA) with 10% serum was then added to stop the reaction. The

cells were then filtered before centrifuged for 5 minutes at 18^{o}C at 1000 rpm. The supernatant was cleared and resuspended in DMEM/F12 (Sigma, USA) with 1xN2 (Gibcol, USA) and 10% fetal bovine serum (Clontech, USA). Culturing of the cells at 37^{o}C was done in an incubator. After 24 hours culturing, change the culture medium. Cytosine-D-arabino-furanoside (AraC; 25 mM; Sigma, USA) was added to the medium to prevent glial proliferation. Patch recording was done after 3-5 days of culture for sodium channel recording.

2.2 HEK293 culturing

The HEK293 cell line was used to express recombinant NMDARs (NR1/NR2B). The cells were cultured in Dulbecco's Modified Eagle Medium (DMEM; Gibcol, USA) with 10% fetal bovine serum (Clontech, USA). Cells were grown exponentially as a monolayer in T75 flasks at 37^{o}C in a humidified 5% CO_2 incubator. When the cells growth reached at approximately 80-90% confluence, they were passaged. Following is the protocol for passaging the cell line:

a. Rinse the cells with 5ml PBS;
b. Trypsinize the cells with 2 ml trypsin-EDTA for 3 min;
c. Add 8 ml fresh media to the trypsinized cells and mix well;
d. Transfer 1 ml trypsinized cells into a new flask containing 15 ml fresh media and return to the 37^{o}C incubator.
e. For the purpose of electrophysiological experiments, transfer 0.2-0.3 ml trypsinized cells into each 35 x 10 mm cell culture dishes containing 2 ml

fresh media and put into the 37°C incubator.

2.3 Preparation of competent cells

(1) Inoculate one single colony into a 4ml LB medium & grow it overnight at 37℃

(2) Use the culture to inoculate the cells at a ratio of 1:10 in LB, and grow it at 37℃ with moderate agitation until the cell density is about OD 0.5-1.0(600nm)

(3) Collection the cell into 50ml Falcon tube and chilling on ice for 10-15minutes

(4) Pellet the cells by centrifugation at 700-1000g (2000-3000rpm) for 12-15min at 4℃. Draining the supernatant and dry the pellet by inverting the tube on paper towels

(5) Resuspending the pellet by moderate vortexing in a volume of RF1 that is 1/3 of the volume collected; incubate the cells on ice for 15 mins (for DH5α) or 1 hour (for HB 101)

(6) Centrifuging the cells at 750-1000g for 12-15mins at 4℃, draining the supernatant, drying by inverting the tube on paper towels.

(7) Resuspending the cells in RF2 to 1:12.5 of the original volume, incubate the cells on ice for 15mins

(8) Aliquot into chilled Eppendorf tubes (100-200ul each)

(9) Deeply frozen in liquid nitrogen, then place at -70℃

RF1: 100mM RbCl 12g

50mM MnCl2.4H2O 9.9g

30mM KAc 30mL (1M)stocking

10mM Cacl2.2H2O 1.5g

15% (W/V) Glycerol 150g

Adjust the pH to 5.8 with acetic acid sterilize by filtration

RF2: 10mM MOPS 20ml (0.5M stock)

10mM RbCl 1.2g

75mM CaCl2.2H2O 11g

15%(W/V) glycerol 150g

Adjust pH to 6.8 with NaOH and sterilize by filtration

2.4 Preparation of Plasmid DNA

A. Preparation of E.coli

50-100μg/ml antibiotic (working station)

LB media 100ml add E.coli and 100μg Amp 37℃ culture overnight

(high copy number plasmid)

B. Production of a cleared lysate

(1) 1-5 ml(high copy number plasmid) centrifuge 5 mins 10,000*g pour off the supernatant & blot the inverted tube on paper towel to remove excess media

(2) Add 250ml cell resuspension solution completely resuspend the cell pellet by vortexing or pipetting

(3) Add 250ul of cell Lysis solution & mix by inverting 4 times (do not vortex).

Incubate until the cell suspension clears, about 1-5 minutes

(4) Add 10μl of Alkaline Protease Solution and mix by inverting 4 times(do not vortex). Incubatefor 5 mins at room temperature

(5) Add 350ul Neutralization Solution and immediately mix by inverting tube 4 times

(6) Centrifuge the bacterial lysate at 14,000g in a microcentrifuge for 10 mins at room temperature.

C. Plasmid DNA isolation and purification (2ml collection tube)

(1) About 850μl cleared lysate was transferes to spin column. Avoid disturbing or transfer any of the white precipitate with the supernatant

(2) Centrifuge the supernatant at 14,000*g for 1min, remove the spin column from the tube and reinsert the spin column into the collection tube

(3) Add 750ml of column wash solution with 95% ethanol to spin column

(4) Centrifuge at maximum speed for 1min, remove the spin column from the tube and discard the floe through. Reinsert the spin column into collection tube

(5) Repeat the wash procedure using 250μl of column wash solution.

6 centrifuge 14,000*g 2mins

(7) Transfer the spin column to a new sterile 1.5ml microcentrifuge tube, being careful not to transfer any of the column wash solution with the spin column. If the spin column had column wash solution associated with, centrifuge again for 1 min

(8) Transfer the spin column to a new sterile 1.5ml microcentrifuge tube

(9) Elute the plasmid DNA by adding 100µl of Nuclease-free water to the spin column. Centrifuge at 14,000*g for 1min

(10) After eluting the DNA, remove the assembly from the 1.5ml microcentrifuge tube

(11) DNA is stable in water without addition of the buffer if stores at -20℃ or below. DNA is stable at 4℃ in TE buffer: add 11ul of 10*TE buffer to the 100ul eluted DNA

(12) Cap the microcentrifuge tube and store the purified plasmid DNA at -20 ℃ and below.

2.5 Transformation

(1) Incubate cell (100µl) & plasmid mix on ice for 20min

(2) Heat shock in 37℃ water bath for 5min

(3) Add 400µl LB into cells

(4) Incubate cells with shaking of 200rpm at 37℃ for 45min

(5) Take out 100ul for plating, about 12-16 hours

Then select several clones of bacteria, and then do PCR to determine if there are inserts in the clone of ligation plate

Method: 10 clones from ligation plates chosen and 2 clones from NC plates

Reagent	volume
10*PCR Buffer	2µl
DNTP(10mM)	0.4µl
MgSO4(25mM)	1.2µl

Primer1(ug/ul)	0.2μl
Primer2(ug/ul)	0.2μl
Polymerase	o.2μl
ddH2O	15.8μl

Total 20μl

PCR 94℃ 94℃ 55℃ 72℃ 68℃ 4℃

2min 30s 30s 1min 7min

40 cycles

2.6 DNA transfection and transient expression

HEK 293 cells were transfected using the modified calcium phosphate precipitation method of Chen and Okayama (1987, 1988). This is a highly efficient method to obtain stable transformation of mammalian cells with supercoiled plasmid cDNAs. The general idea is to allow a calcium phosphate-cDNA co-precipitate to form in the tissue culture medium during prolonged incubation (15-24 hours) under controlled conditions of pH (6.96) and CO_2 tension (3%). The transfection solutions used in this procedure were prepared as follows: (1) 2 x BES-buffered saline containing (in mM): 50 BES, 280 NaCl, 1.5 $Na_2HPO_4 \cdot 2H_2O$, pH 6.96 with HCl at room temperature; (2) 2.5 M $CaCl_2$. The water used to make the transfection solution was sterilized and deionized with resistance of 18 MΩ · cm (Millipore, USA). The solution was sterilized by passage through a 0.22-micron filter.

The cDNA to be used for transfection was derived from maxipreps of plasmids constructs containing the NMDA receptor subunits NR1 and NR2B. The protocol for

transfection is as follows:

(1) As described in Section 2.2, transfer the cells to be used for patch-clamp experiments onto 35x10 mm tissue culture dishes 24 hr before transfection;

(2) Dilute 2.5 M $CaCl_2$ to 0.25M;

(3) Mix 1μg cDNA with 200μl 0.25M $CaCl_2$ and add 200μl of 2xBES-buffered saline;

(4) Incubate the mixture for 5-10 min at room temperature before applying to cells;

(5) Add the $CaCl_2$/DNA and 2xBES-buffered saline solution dropwise to dishes of cells, swirling gently to mix well;

(6) Incubate the cultures for 15-24 hr at 37^{o}C in a humidified incubator at 3% CO_2;

(7) Rinse the cells with fresh media, add 2 ml fresh media into dishes and return to the 5% CO_2 incubator.

The efficiency of transfection was monitored by the formation of fine granulated particles precipitate on the cells. Too little precipitate indicates that insufficient cells are transfected and too much is generally toxic. If too much precipitate was present, it could be reduced by lowering the PH slightly (in 0.05 pH increments). The patch-clamp studies were conducted over the following 24-72 hr.

2.7 Patch-clamp Electrophysiology

2.7.1 Patch pipettes preparation and Solutions

Borosilicate glass electrodes were pulled using flaming/brown pipette puller from Sutter Instruments Company (Model P 97) and they have a resistance of 3-5 MΩ when filled with standard intracellular solution. Whole-cell patch configuration was obtained from Swiss albino cortical neurons and HEK293 cell line using the glass electrodes filled with pipette solution containing (in mM):

a. 140 Gluconic acid, 5 HEPES·Na, 4 NaCl, 2 $MgCl_2$, 0.5 $CaCl_2$, and 5 EGTA, pH7.4 with NaOH for NMDA channel recording;
b. 145 CsCl, 2.8 NaCl, 2 MgCl2, 10 HEPES·Na, 2 EGTA, 2 ATP and 0.1 MgGTP, pH 7.4 with C_sOH for sodium channel recording.

The neurons were placed in an external bath solution containing (in mM):

a. 150 NaCl, 10 HEPES·Na, 1 $CaCl_2$, 3 KCl, 10 Glucose, pH7.4 with HCl (NMDAR recording);
b. 145 NaCl, 2.8 KCl, 2 MgCl2, 2 CaCl2, 10 HEPES, pH 7.4 with NaOH (Sodium channel recording).

2.7.2 Microscope, Amplifier and recording chamber

The cells were observed under Axiovert 200 microscope (Zeiss, German) at 10X magnification. Signals were recorded using HEKA EPC 9 triple patch-clamp amplifier. The starting holding potential was set to zero, and once the patch was broken, the holding potential was set to –60 mV and -100mV for NMDAR and sodium channel recording, respectively.

During the experiment, the bath solution was continuously perfused into a small

volume recording chamber (2ml). A ground electrode consisting of an Ag^{+}/AgCl wire was placed in the chamber. The patch pipette holder was also fitted with an Ag^{+}/AgCl wire electrode. Both electrodes were periodically re-chlorided by placing in a $FeCl_3$·HCl solution for 30-60 min. All experiments were conducted in voltage-clamp configuration.

2.7.3 Whole cell recording

The whole cell configuration was established by the following procedure. Coverslips attached cultured transfected Hek293 cells or cortical neurons were transferred into recording chamber that was continuously superfused with the standard bath solution. After placing the pipette into bath solution, voltage of 5 mV was applied to estimate the pipette resistance. Those pipettes with resistances that were out of 3-5 MΩ were discarded. The pipette tip was gently placed on the cell surface and suction applied. Upon the formation of a high-resistance cell-attached seal (>1 GΩ), the membrane enclosed by the pipette tip was ruptured by the application of further suction to obtain the whole cell mode. Establishment of the whole-cell recording configuration was indicated by a slight increase in background noise and an increase in amplitude of the capacitative transient. Then the -60 mV and -100mV membrane holding potentials were slowly applied for NMDAR and sodium channel recording, respectively. Then experimental recording started.

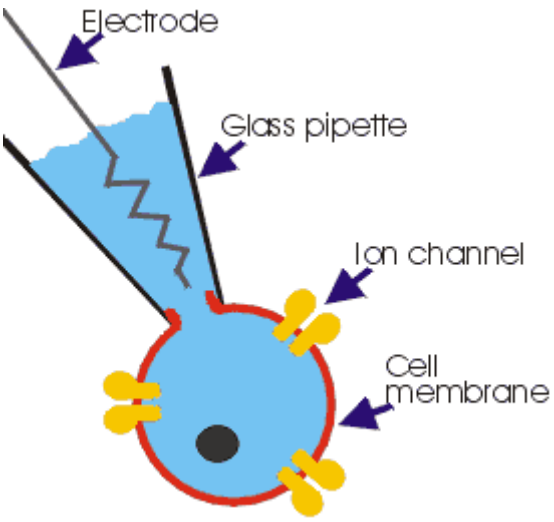

Fig. 7. WHOLE CELL RECORDING: When apply suction to the back of the pipette to break the cell membrane, you enter the "whole cell" recording mode. In this configuration the pipette solution and the cell interior become contiguous

2.8 RT-PCR

First-strand cDNA synthesis was performed with the SUPERSCRIPT First-Strand Synthesis Kit (Invitrogen, USA). First, the total RNA and primer mixtures were prepared in 0.5 ml tubes, containing 5 µg total RNA, 10 mM dNTP mix 1 µl, oligo (dT) (0.5 µg/µl) 1 µl and DEPC-treated water. The samples were incubated at 65 ºC for 5 minutes to denature and were placed on ice for 5 minutes. Then the reaction mixture was prepared containing 10 × RT buffer 2 µl, 25 mM $MgCl_2$ 4 µl, 0.1 M DTT 2 µl and RNaseOUT Recombinant RNase Inhibitor 1 µl. 9 µl of reaction mixture was added to each RNA/primer mixture and incubated at 42 ºC for 2 minutes to anneal and 1 µl (50 units) of SUPERSCRIPT II RT was added to each tube and incubated further at 42 ºC for 50 minutes to synthesize the cDNA. The reaction was terminated at 70 ºC for 15 minutes and chilled on ice. The reaction was collected by brief centrifugation, and was

added 1 µl of RNaseH to each tube and incubated for 20 minutes at 37 ºC before proceeding to do PCR.

2.10 Neurogranin peptides with phosphorylated (PhosIQ) and unphosphorylated (UnPhosIQ) IQ motif.

100 µM neurogranin peptides containing phosphorylated and unphosphorylated IQ motif (PhosIQ and UnPhosIQ respectively) were added to the pipette solution in separate experiments. When the patch was broken during whole cell recording, the peptides will diffuse through into the cell. Whole-cell recordings were done over a period of time from the onset of patch break where the peptides are allowed to slowly diffuse into the cell.

Ng peptides (BioGene, German) used:

(1) With phosphorylated IQ motif phosphorylated at the serine site (PhosIQ):

C A K I Q A p**S** F R G H M

(2) With unphosphorylated IQ motif (UnPhosIQ):

A A A K I Q A S F R G H

The consensus regarding the sequence of IQ motif is IQXXXRG (X represents any amino acid); therefore though here the sequences of these two IQ peptides are not identical, the small differences at each end have no significant effect on their binding with CaM.

2.11 Data analysis

The data were converted from Pulsefit 8.0 software to Igor-Pro 4.0, SPSS 11.0 or Sigma plots for data analysis, and were plotted for each group. Data were presented as

means ± S.E.M. each group. Statistical analysis was performed using one way ANOVA followed by Tukey's post-hoc analysis. A level of $P < 0.05$ was considered significant.

RESULTS

3.1 Ng peptide modulates the properties of sodium channel in a CaM-dependent manner

Voltage-gated sodium channels (NaChs or VGSCs) initiate the fast upstroke of action potentials in both nerve and muscle cells. Modulation of VGSCs can have a major impact on cell excitability and regulate the function of brain. Recent studies suggest that the activity of sodium channel proteins is regulated by calmodulin that is expressed in virtually all eukaryotic cells. CaM can induce changes in sodium channel proteins via its binding per se and in response to changes in intracellular Ca^{2+} concentration (Chin and Means, 2000). Schultz et al. (Schultz et al., 2000) identified IQ motif, the CaM binding motif (see Introduction 1.3.3), in the C termini of $Na_v1.1$-1.9, all of the known members of VGSCs family (Fig 8).

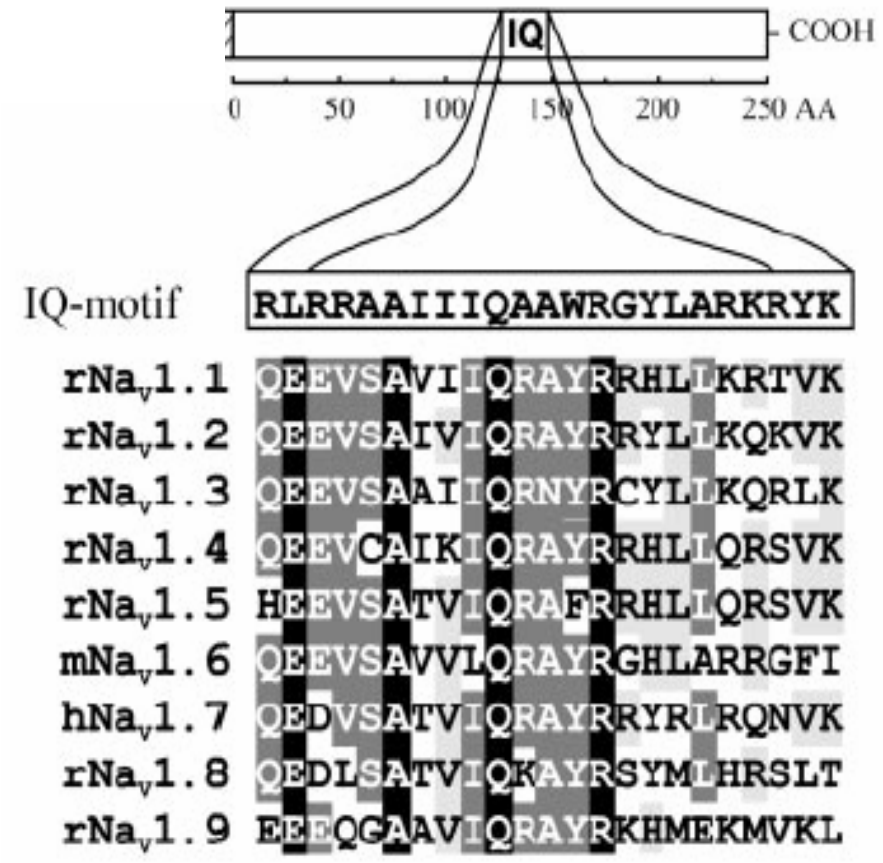

Figure 8. Alignment of IQ motifs within VGSC C-termini. Identical and highly conserved residues are shaded in black and gray, respectively. Shown is a schematic of a GST-fusion protein with the 250-amino-acid-long C terminus of a sodium channel, indicating the position of the highly conserved IQ motif (Schultz et al., 2000).

Experiments that used GST-fusion proteins consisting of the whole C termini of all of the known members of the VGSCs family showed that $Na_v1.2$, $Na_v1.3$, $Na_V1.4$, $Na_v1.6$ exhibited strong binding to CaM under both high and low calcium conditions, while $Na_v1.5$, $Na_v1.7$-1.9 did not (Herzog et al., 2003).

On the other hand, Ng also contains IQ motif and functions as a regulator of the availability of CaM, either by sequestering CaM to limit its abundance in the cytoplasm, or by acting as a source of CaM (Gerendasy et al., 1994), by keeping it localized in specific regions of the cytoplasm such as in growth cone membrane of neurons (Liu and Storm, 1990). So the idea that Ng might act as the mediator of VGSCs by competing with channel protein to bind CaM seems rather obvious.

To investigate whether Ng can modify the functional properties of sodium channels ($Na_v1.3$) on primary cortical neurons from 0-2 day Swiss Albino mice (Fig.9), we perfused two Ng peptides into neuronal cell bodies: one is PhosIQ (CAKIQAp**S**FRGHM) phosphorylated at the serine site within its IQ motif; while another one is UnPhosIQ (AAAKIQASFR) containing unphosphorylated IQ motif. As mentioned above, the phosphorylated Ng binds CaM poorly, compared to unphosphorylated one. 100 μM of each Ng peptide was added to the pipette solution in separate experiments, respectively. When the sucked patch of membrane was broken during whole cell recording, the peptides will diffuse through into the cell. Recordings were done at the onset of patch break, before the peptides diffused into

A.

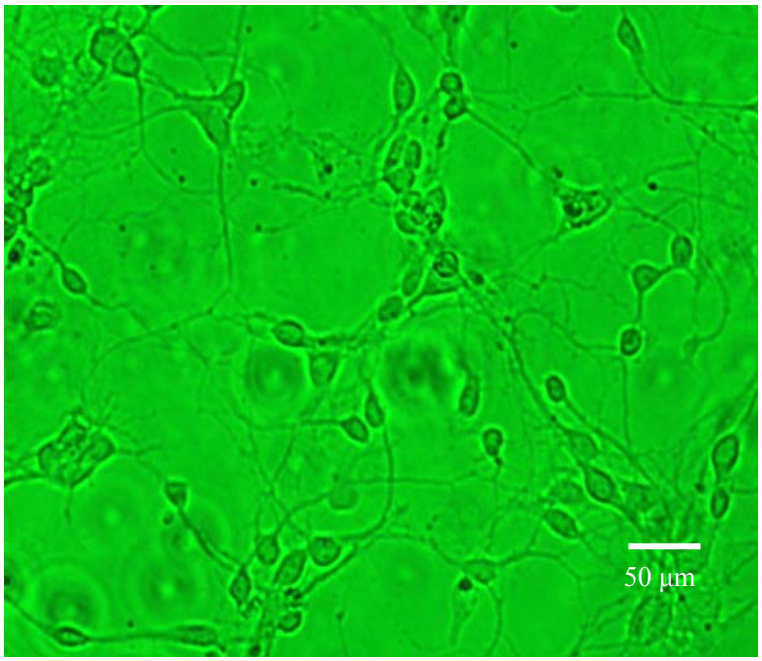

B.

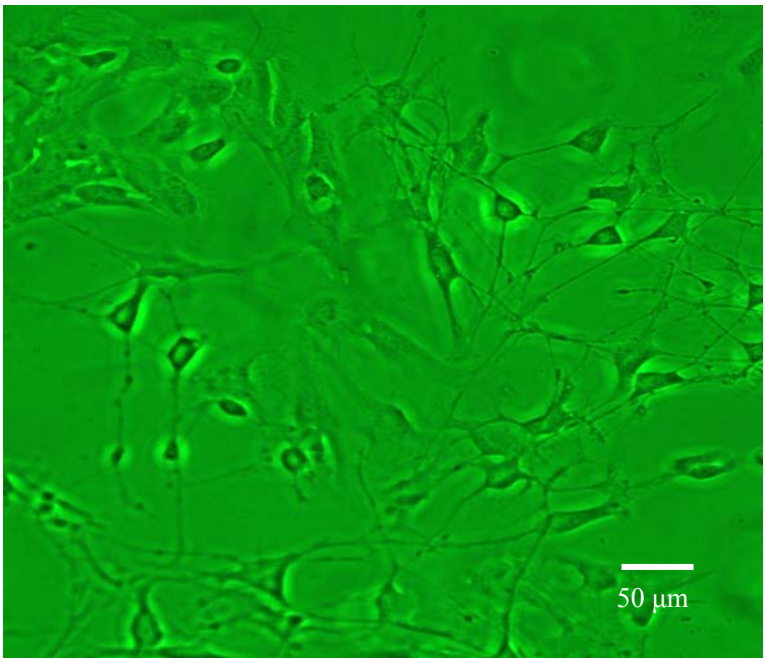

Fig 9. Primary cortical neuron culture. A, 3 days culture after plating; B, 5 days culture after plating. Whole cell patch recordings were done during 3-7 days culturing.

the cell as control; and were done over a period of time from the onset to allow the peptides to diffuse slowly into the soma.

The sodium currents produced by neurons perfused with UnPhosIQ (Fig. 10 and 11) were suppressed by >30% (n=11). In contrast, the neurons perfused with the phosphorylated peptide PhosIQ produced currents that did not vary with time. Since, firstly, CaM binds to Ng *in vivo*; secondly, CaM is the only Ng-interacting protein isolated from brain cDNA libraries; thirdly, phosphorylated Ng binds CaM poorly, these data suggest Ng peptide may initiate sodium currents reduction in a CaM dependent manner. Furthermore, as shown in Fig 11, the sodium currents in neuron before peptides infusion activated at ~-50 mV, peaked at ~-20mV, and had reversal potentials close to that predicted by the Nernst equation:

$$E_{Na} = 2.303\frac{RT}{F}\log_{10}\frac{[Na]_o}{[Na]_i} \quad (\sim 55.6 \text{ mV}).$$

However, though reversal potentials remained same, the currents peaked close to ~-35 mV after infusion of PhosIQ. No such changes occurred in the currents of cells infused with UnPhosIQ.

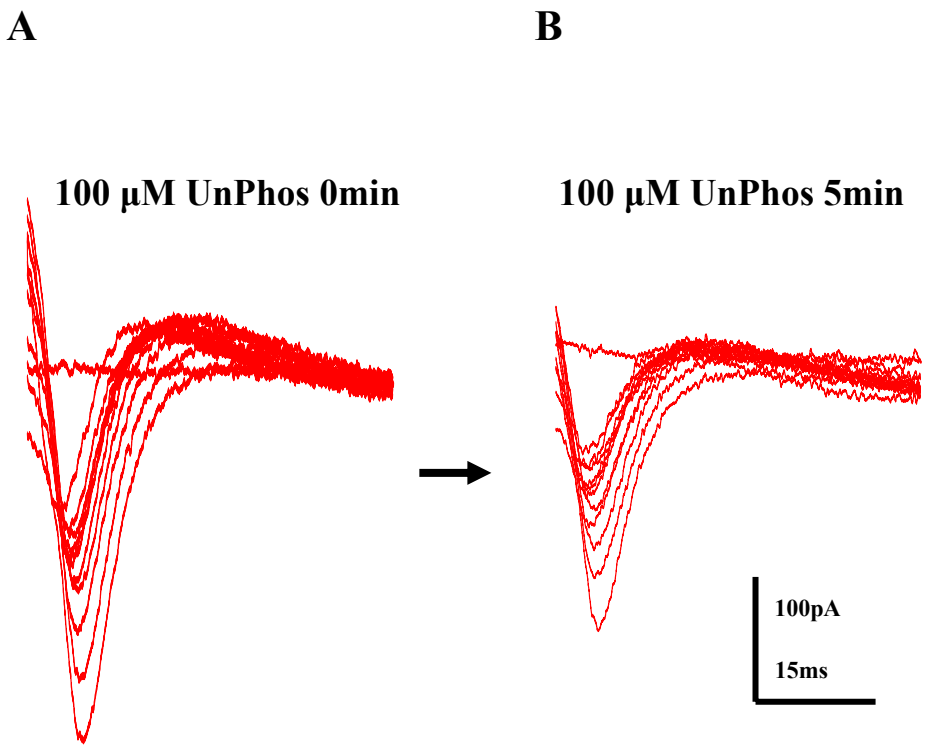

Fig. 10. Sodium channel currents from cortical neurons are suppressed by infusion of 100µM UnPhosIQ, a Ng peptide containing unphosphorylated IQ motif. The Na^+ currents were elicited by depolarization from -100 mV (holding potential) to potentials between -50 mV and 60 mV in 10 mV increments. **A:** The currents were recorded at 0 min of whole cell recording and before intracellular perfusion of UnPhosIQ. **B**: The currents recording at 5 min after peptide perfusion. Dose-dependent studies show that the effect of UnPhosIQ reaches peak at 100 µM (Data not shown).

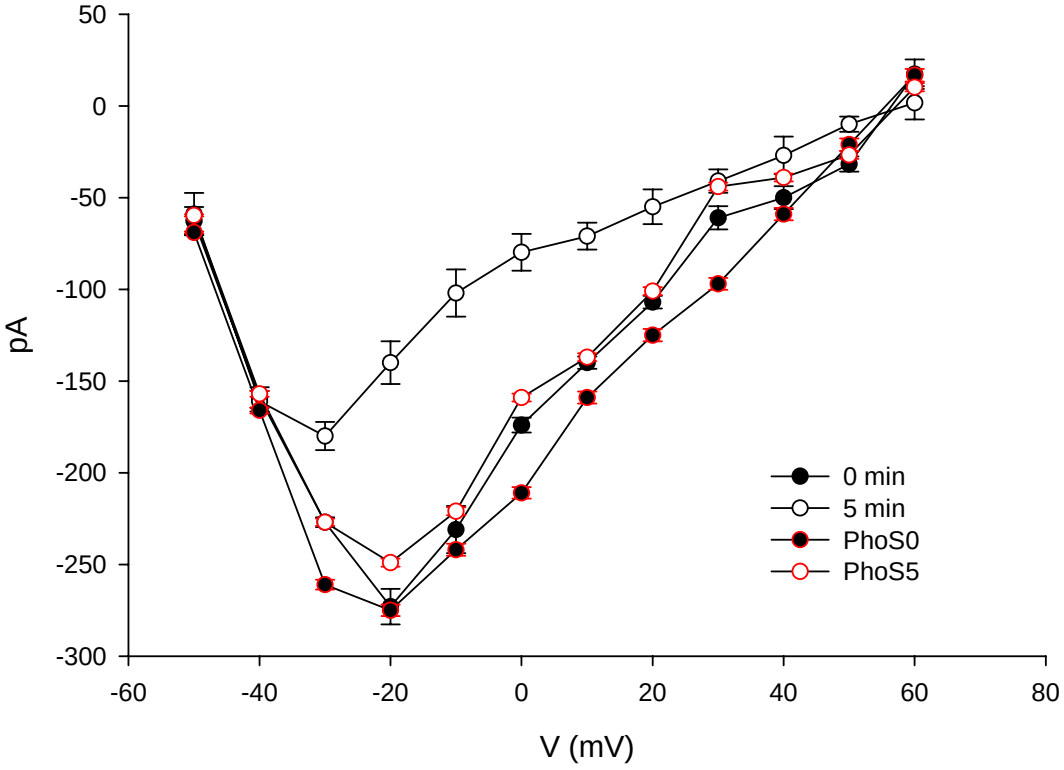

Fig 11. Sodium current-voltage relationship for neurons infused with peptides UnPhosIQ or PhosIQ. Recordings were done before and after (5min) peptides infusion. The sodium currents produced by neurons perfused with UnPhosIQ were reduced by >30%. While the neurons perfused with the phosphorylated peptide PhosIQ produced currents that did not vary with time.

Infusion of Ng peptides also resulted in significant ($P<0.05$) shifts in the voltage dependence of activation (Fig.12) and steady-state inactivation (Fig.13). The voltage dependence of activation was determined from the peak sodium current recorded during 100-msec voltage steps from -100mV to potentials between -50 mV and +60 mV. Conductance (G) was calculated from peak current (I_{peak}) according to $G = I_{peak} /(V_{step}-V_{Na})$, where V_{step} is the step potential and V_{Na} the measured reversal potential. Steady-state inactivation was assessed using a holding potential of -100 mV, a 200-msec pre-pulse to potentials between -100 mV to 0 mV, and a test pulse to 0 mV. Normalized conductance-voltage curves and steady-state inactivation curves were fit with a Boltzmann function:

$$\frac{G}{G_{\max}} = \frac{1}{1+e^{(V_{step}-V_{0.5})/k}}$$

Where $V_{0.5}$ is the midpoint of the curve and k is the slope factor. The midpoints for activation were not significantly different for currents recorded before (-25.9±0.1mV; n=6) and after PhosIQ perfusion (-26.5±1.0 mV; n=8). However, perfusion of UnPhosIQ resulted in significant ($P<0.05$) shifts in the voltage dependence of activation and steady-state inactivation. This included hyperpolarizing shifts of ~20 mV (from -23.9±0.6 mV; n=5 to -43.7±0.4 mV; n=7) in the midpoints of the normalized sodium conductance curves for activation with noticeable changes in slope (from 6.5±0.4; n=5 to 10.9±0.5). For steady-state inactivation, there were hyperpolarizing shifts of ~15 mV (from -43.1 mV; n=6 to -59.7 mV; n=8) in the midpoints of the conductance curves.

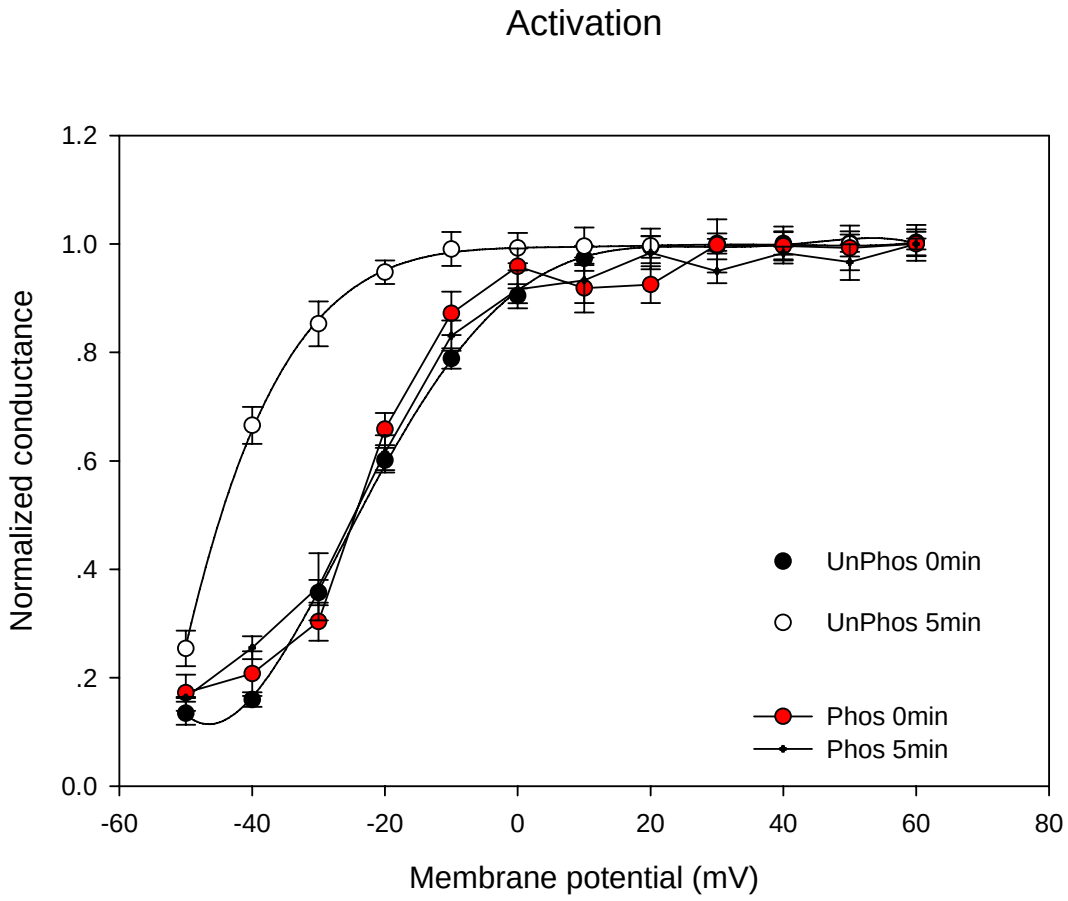

Fig 12. Hyperpolarizing shifts in the voltage dependence of Na^+ channel activation upon cells perfused with UnPhosIQ. The voltage dependence of activation was determined from the peak sodium current recorded during 100-msec voltage steps from -100mV to potentials between -50 mV and +60 mV. Mean normalized voltage-conductance relationships were fitted with Boltzmann functions, with $V_{0.5}$ as the midpoint and k the slope factor. In each case n=5-9 cells. UnPhos 0 min: $V_{0.5}$= -23.9±0.6 mV, k=10.9±0.5; UnPhos 5 min: $V_{0.5}$= -43.7±0.4 mV, k=6.5±0.4; Phos 0 min: $V_{0.5}$= -25.9±0.1 mV; Phos 5 min: $V_{0.5}$=-26.5±1.0 mV

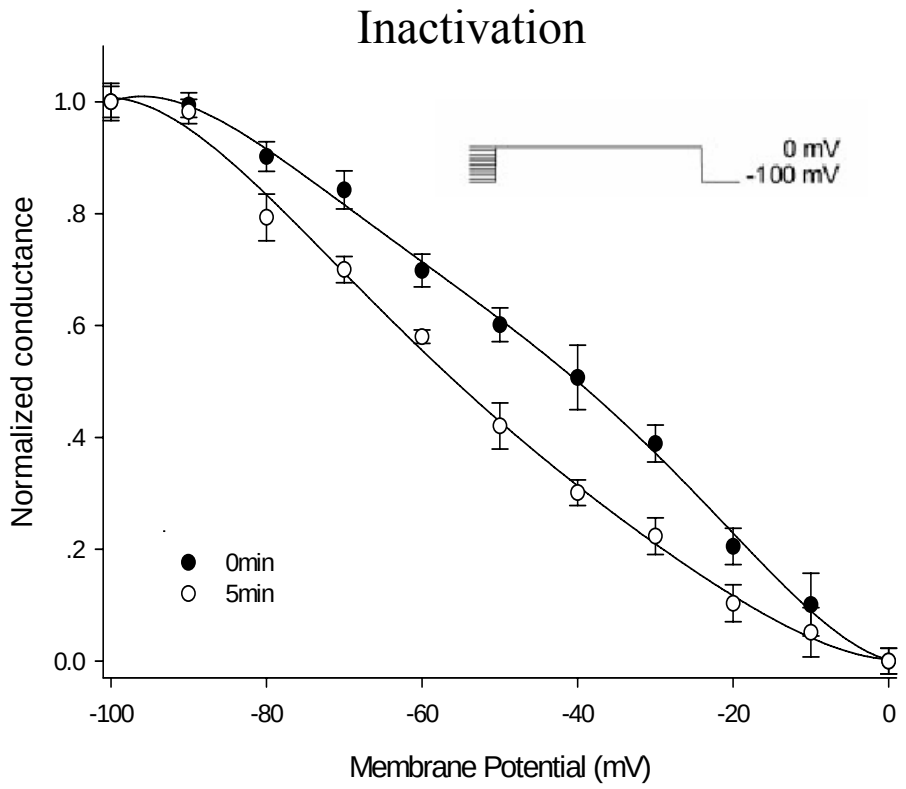

Fig 13. Hyperpolarizing shifts in the voltage dependence of Na^+ channel inactivation upon cells perfused with UnPhosIQ. Steady-state inactivation was assessed using a holding potential of -100 mV, a 200-msec pre-pulse to potentials between -100 mV to 0 mV, and a test pulse to 0 mV. Mean normalized voltage-conductance relationships were fitted with Boltzmann functions, with $V_{0.5}$ as the midpoint. In each case n=6-8 cells. UnPhos 0 min: $V_{0.5}$= -43.1±2.6 mV, k=17.2±2.0; UnPhos 5 min: $V_{0.5}$= -59.7±0.4 mV, k=18.7±1.7.

Although the activation time constant τ_m did not differ between before and after UnPhosIQ perfusion, there was a significant difference (Student's *t* test, $P<0.05$) in the inactivation time constant τ_{fast} between them (Fig. 14). The rate of fast inactivation was determined here by fitting the current record at -30 mV (from 90% I_{max} to the end of the 15-msec step) with the sum of two exponentials:

$$I_{(t)} = A_0 + A_1(\exp[-t/\tau_{fast}]) + A_2(\exp[-t/\tau_{slow}])$$

where A_0 is a constant, A_1 and A_2 are the fractions of the fast and slow inactivating components, and τ_{fast} and τ_{slow} the time constants of the fast and slow inactivating components. As shown (Fig. 14), the perfusion of Ng peptides UnPhosIQ slowed the sodium channels in cortical neurons by 21% at -30 mV.

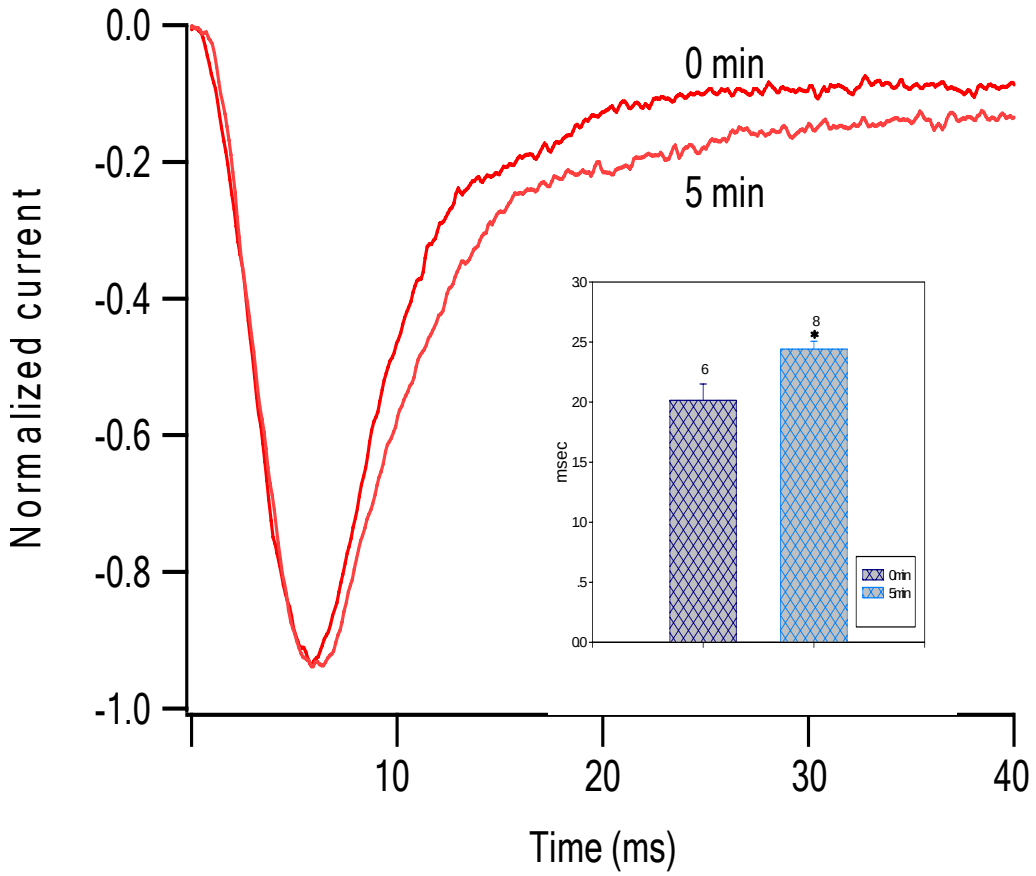

Fig 14. Normalized Na^+ currents elicited by depolarization from -100 mV to -30 mV upon cells perfused with UnPhosIQ. The current recorded 5 min after UnPhosIQ perfusion displayed slower kinetics. Inset: Percentage of the current decay that can be accounted for by a fast exponential component with a time constant of 2.01±0.06 msec for before UnPhosIQ perfusion and 2.44±0.06 msec after perfusion.

3.2 The function of Ng peptides in the regulation of NMDA channel current

The *N*-methyl-D-aspartate (NMDA)-type glutamate receptor is a major source of Ca^{2+} influx into neurons in the central nervous system. NMDA receptors in the cerebral cortex largely consist of two NR1 and two or three NR2A and 2B subunits, which are homologous to each other. Each subunit has an extracellular N terminus, four membrane regions (M1–4), and an intracellular C terminus. M1, M3, and M4 are transmembrane regions but M2 loops into and back out of the plasma membrane at its cytoplasmic face (see Introduction). The C-terminal domain of NR1 contains the 30 residue-long membrane-proximal C0 region common to all NR1 isoforms, followed in some NR1 isoforms by the C1 region (37 residues), which can be spliced in or out, and by either the C2 (38 residues) or the C2' (22 residues) region, which is downstream of C2 in the genome. The C2 region can be spliced out, but, when present, C2' will not be translated because C2 carries its own stop codon.

In a negative feedback loop calmodulin (CaM) inhibits Ca^{2+} influx through the NMDA receptor by strongly binding to the NR1 C0 region in the presence of Ca^{2+} (Ehlers et al., 1996; Zhang et al., 1998). The same region interacts with α-actinin, which can be displaced by Ca_4^{2+}-CaM (Wyszynski et al., 1997). Displacement of α-actinin appears to reduce NMDA receptor activity by increasing the calcium dependent inactivation (CDI), *i.e.* closing of the receptor pore while the glutamate is still present (Krupp et al., 1999). The Ca_4^{2+}-CaM -mediated negative feedback mechanism may help to reduce the otherwise uncontrolled Ca^{2+} influx through the NMDA receptor during ischemia as occurs during stroke and other pathological

conditions (Lee et al, 1999). Ischemia triggers a massive release of glutamate from neurons, which results in overactivation of NMDA receptors. The ensuing unchecked Ca^{2+} influx ultimately leads to neuronal dysfunction and death.

CaM constitutes the major Ca^{2+} sensor in eukaryotes and is ubiquitously expressed. It spans 148 residues and consists of an N- and a C-terminal domain, each containing two EF-hand Ca binding sites (I–IV). Ca^{2+} binds cooperatively, with sites III and IV in the C-domain usually having a 10-fold higher affinity than sites I and II in the N-domain. Ca^{2+} binding induces rearrangement of the tertiary structure of each domain, stabilizing the exposure of hydrophobic clefts. These surfaces promote the association of CaM with a wide array of target proteins including kinases, phosphatases, ion channels, esterases, and metabolic enzymes (Hoeflich et al., 2002).

On the other hand, CaM binds to the IQ motif of Ng in a Ca^{2+}-sensitive manner, namely, Ng forms a complex with CaM in the absence of Ca^{2+} , and the complex disassociates in the presence of Ca^{2+} (Baudier et al, 1991; Huang et al, 1993; Gerendasy et al, 1995). So, in this study we focused on the roles of Ng in NMDA receptor signaling and tried to verify whether the effect of Ng is through CaM/Ng complex, if any.

The general approach to investigate the interaction of NMDA receptor was to apply Ng peptides into intracellular plasma, and to analyze the function of NMDA receptor using patch-clamp electrophysiology. To investigate whether Ng can modify the functional properties of NMDA receptor channels expressed on HEK293 cells, first step, we transfected HEK cells with NR1 and NR2B plasmids. Each of them

contains an eGFP marker gene and an NR1 or NR2B gene, respectively (Fig. 15), and would give rise to green fluorescence if transfected successfully (Fig. 16). RT-PCR was used to verify both NR1 and NR2B were expressed in Hek293 cells (Fig. 17). Though western blot is also a good option, here RT-PCR is convenient and sufficient.

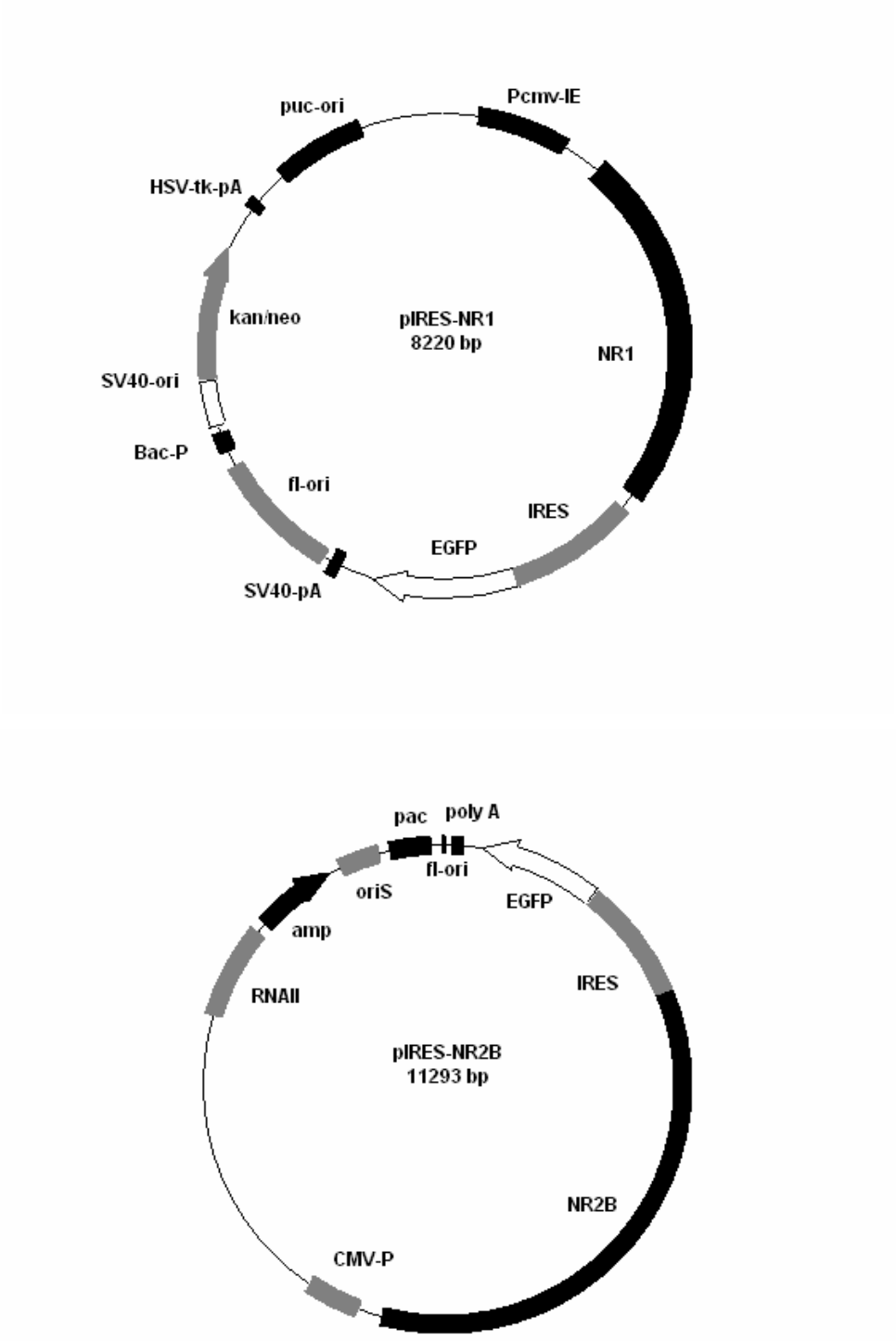

Fig.15 Construct maps of pIRES-NR1 and pIRES-NR2B: both contain an eGFP marker gene and NR1 or NR2B gene. Successful in vitro transfection gives rise to green fluorescence.

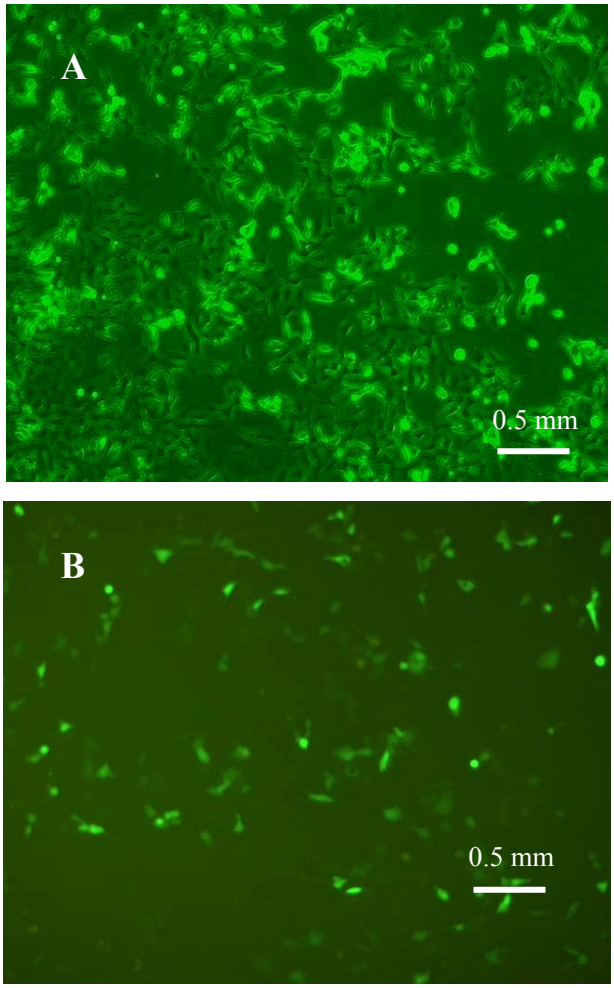

Fig. 16 Hek293 cells transfected with NR1 and NR2B plasmids. A, Culture cells. A mixture of fluorescence and light microscopy image. B, Fluorescence image of transfected cells.

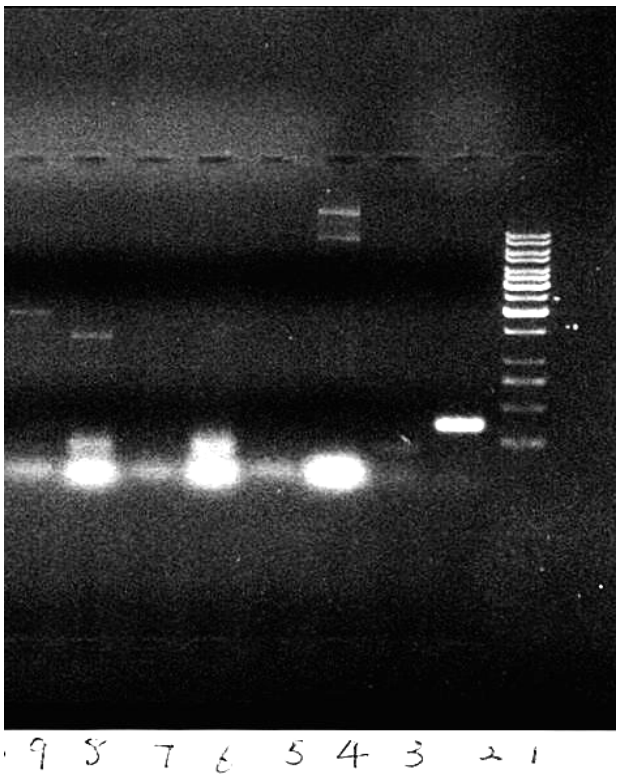

Fig 17. RT-PCR Analysis of NR1 and NR2B expression on HEK293 cells

1: Ladder
2: RT-PCR positive control (positive control provided by SUPERSCRIPT kit);
3: No transfection control
4: Negative control
5: Negative control
6: No RT control;
7: Negative control
8: NR2B;
9: NR1;

Whole-cell NMDA receptor-mediated currents were recorded following the infusion of the Ng peptides, UnPhosIQ and PhosIQ, into NR1/NR2B expressing HEK293 cells (Fig. 18 and 19). The intracellular calmodulin concentrations of HEK cells are estimated to be ~10 μM (Vincenzi and Hinds, 1980), so a relatively high concentration (100μM) of two Ng peptides were used, and whole-cell NMDA currents were monitored for period of 15 min after infusion. This procedure allowed the peptides to sufficiently bind the endogenous intracellular calmodulin. Fast application of glutamate (100 μM in 5S) in a solution containing 50 μM glycine evoked whole cell currents. During the 5S pulses of glutamate to cells expressing NR1-NR2B channels, the inward currents slowly declined (CDI, Fig 18.). The Calcium Dependent Inactivation (CDI) was quantified by:

$$CDI = (I_{pe}-I_{ss})/ I_{pe},$$

where I_{pe} is the peak current and I_{ss} the steady state current measured at the end of the glutamate pulse.

Surprisingly, as shown in Figure 20, intracellular infusion of 100 μM either PhosIQ or UnPhosIQ reduced the CDI of NMDA currents slightly. Moreover, there is no significant difference between the extents of CDI reduction under two scenarios. This result is beyond expectation. Our data is most consistent with a nonspecific action. I will try to give a tentative interpretation to this result in the part of discussion.

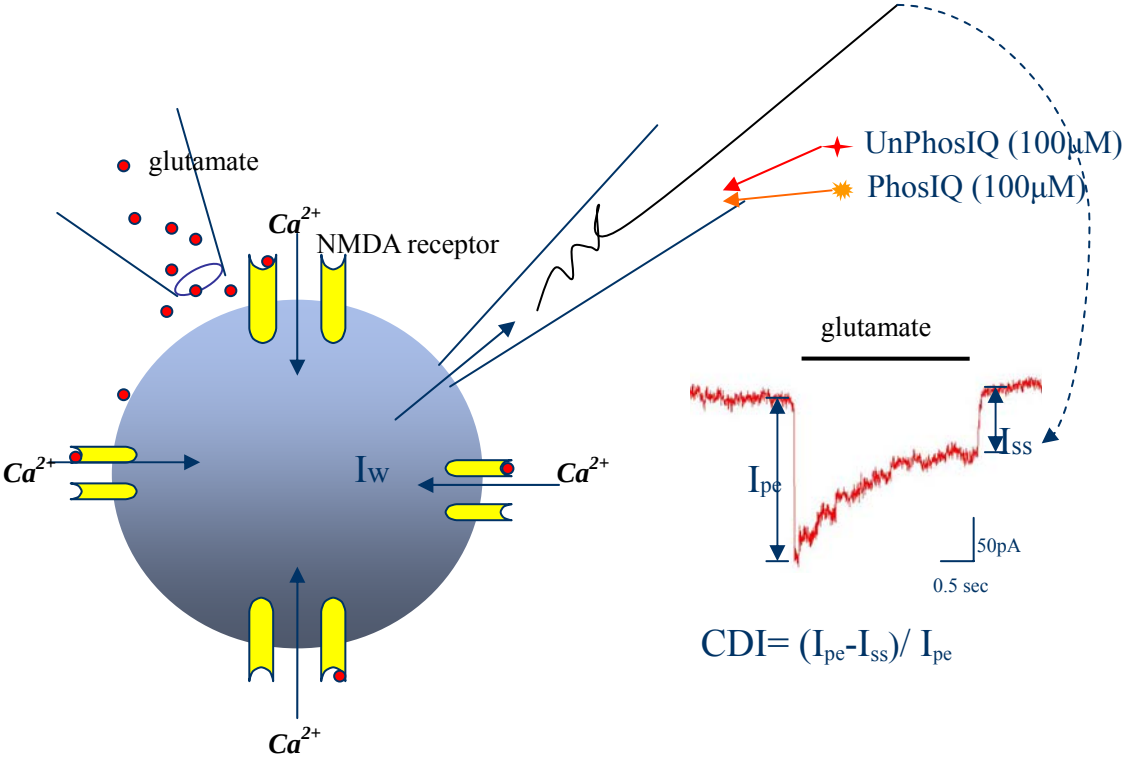

Fig 18. Schematic diagram illustrating Whole Cell Recording on Hek293 cells transfected with NR1\NR2B subunits and the Calcium Dependent Inactivation (CDI) of NMDA channel currents. Two glass pipettes were used here: one was used to apply the agonist-glutamate to the target cell; another was the recording electrode and also was used to perfuse the Ng peptides into the target cell. As shown, the CDI was quantified by: CDI = $(I_{pe}-I_{ss})/ I_{pe}$, where I_{pe} is the peak current and I_{ss} the steady state current measured at the end of the glutamate pulse.

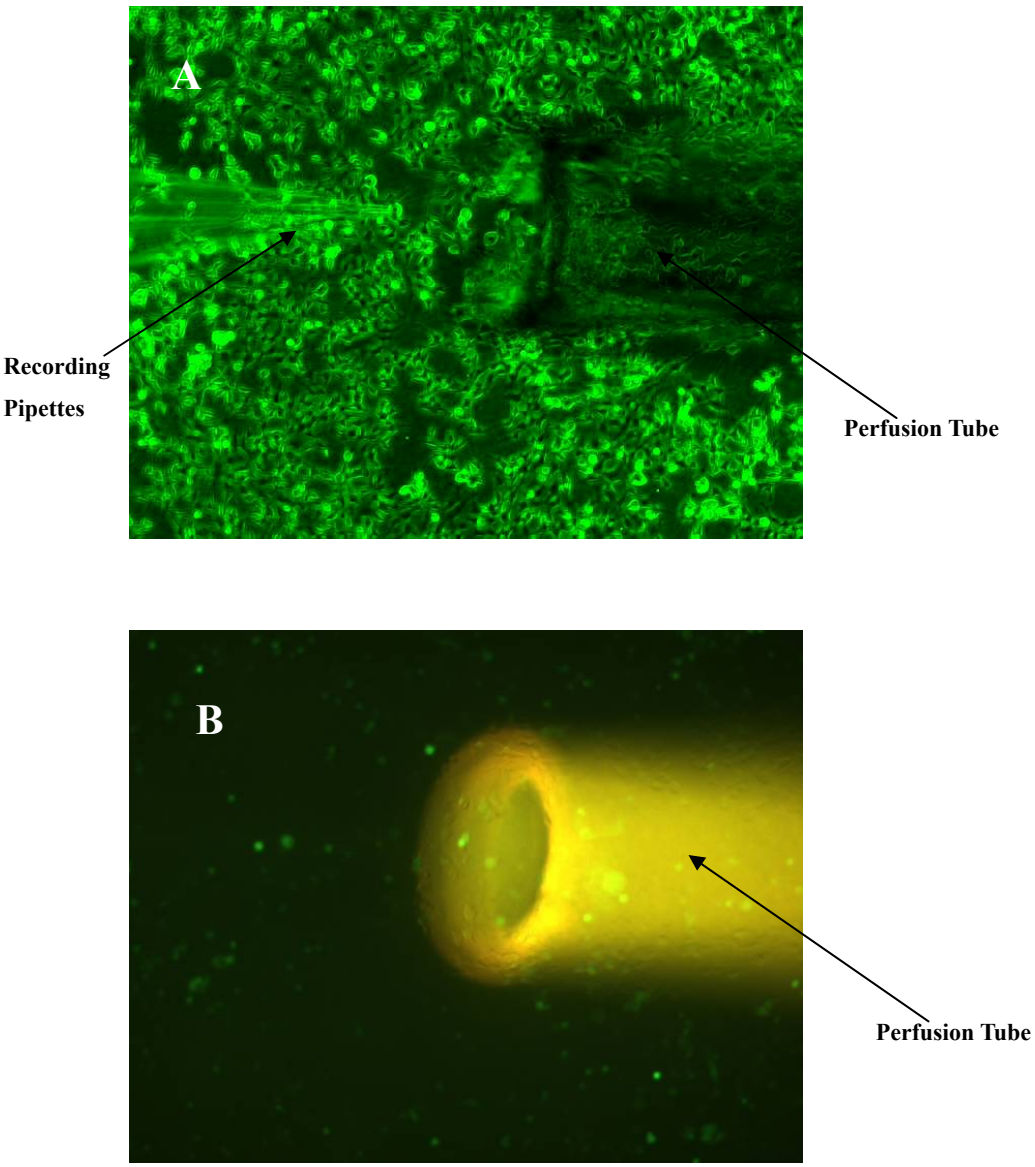

Fig 19. Whole Cell Recording on Hek293 cells transfected with NR1\NR2B subunits. A, Whole Cell Recording under Axiovert 200 microscope at 10x magnification. B, Fluorescence image, can not see recording pipette under the fluorescence lamp.

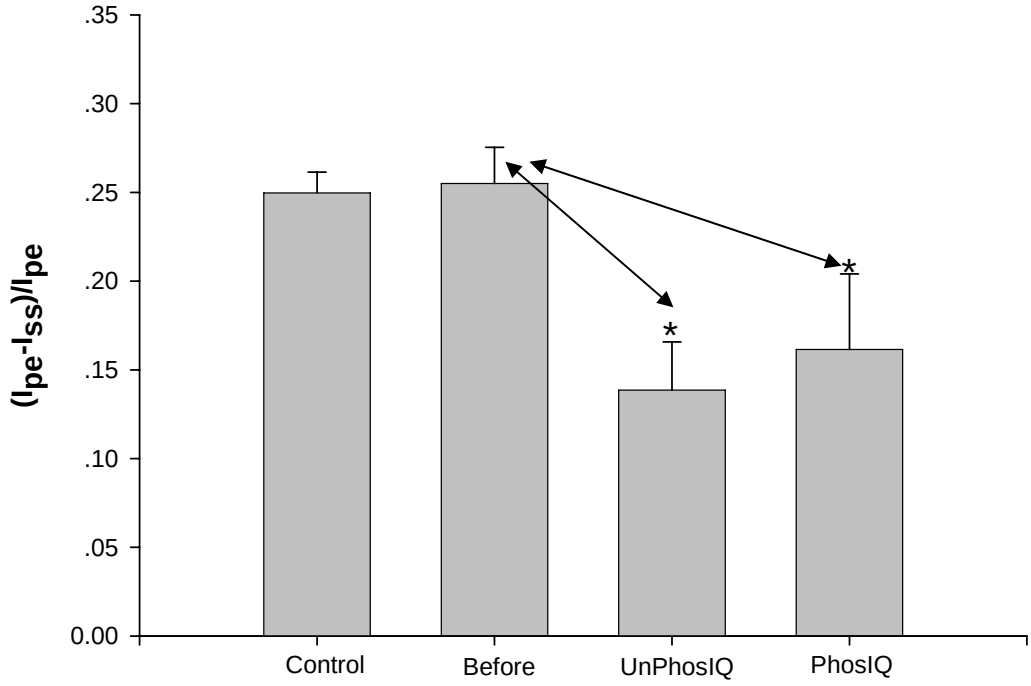

Fig 20. The bar graph shows values of (Ipe-Iss)/Ipe (CDI) before and after intracellular infusion of the UnPhosIQ and PhosIQ. A small decrease of CDI was observed upon intracellular infusion of the UnPhosIQ and PhosIQ, compared to the control, but there is no significant difference between the CDIs of UnPhosIQ group and PhosIQ group (ANOVA with subsequent Tukey test, error bars represent SEM).

DISCUSSION

The activity of many channel proteins is regulated by calmodulin (CaM) (Levitan, 1999; (Saimi and Kung, 2002), a 16.7 kDa protein that is expressed in virtually all eukaryotic cells. CaM can induce changes in target proteins via its binding per se and in response to changes in calcium concentration (Chin and Means, 2000). For example, the activity of sodium channels in *Paramecium tetraurelia* is CaM-dependent (Ling et al., 1992;Saimi and Ling, 1995), and CaM plays a crucial role in the modulation of calcium channels and potassium channels (Ehlers et al., 1996;(Lee et al., 1999); (Peterson et al., 1999); (Zuhlke et al., 1999).

On the other hand, Neurogranin (Ng) is highly concentrated postsynaptically in neuronal cell bodies and dendrites of the cerebral cortex, hippocampus, and striatum(Pak et al., 2000;Watson et al., 1992), and functions as a regulator of the availability of CaM, either by sequestering CaM to limit its abundance in the cytoplasm, or by acting as a source of CaM (Gerendasy et al., 1994), by keeping it localized in specific regions of the cytoplasm such as in growth cone membrane of neurons (Liu and Storm, 1990).

Considering the above two facts, it is worthwhile thinking that different expression levels of Ng may modulate multifold ion channels in neurons in a CaM dependent manner. In this study, we focused on the roles of Ng in both sodium and NMDA receptor signaling. In the study of sodium channels, we recorded the channel currents on cortical neurons; in contrast, we recorded the NMDA channel currents on

Hek293 cell line. This is because: firstly, there are other types of glutamate channels besides NMDA channel in cortical neurons, it is therefore not easy to distinguish the NMDA channel currents from other ones; secondly, NMDA channels are highly expressed only after postnatal 14 days, while our cortical neuron cultures can not last so long. In addition, the cortical neurons from postnatal 14d mice are difficult for culturing.

4.1 Ng, CaM and Sodium Channels

In this study, we described the modulation of the native sodium channels in cultured cortical neurons from Swiss Albino mice of postnatal day 0-2. Since in rodents, $Na_v1.3$ is highly expressed in the nervous systems of fetal and new-born mice, the major component of the currents recording here is $Na_v1.3$ current. And recent papers indicated that $Na_v1.3$ contains an IQ motif and exhibited binding to CaM under both high and low calcium conditions (Herzog, 2003). We showed that the functional expression of VGSCs current is critically dependent on the ability of Ng peptides to bind CaM, because the effect of Ng peptides on VGSCs disappeared when the site of serine within its IQ motif was phosphorylated and the peptides lost the binding ability to CaM. The sodium currents produced by neurons perfused with UnPhosIQ were reduced by >30%, while the neurons perfused with the phosphorylated peptide PhosIQ produced currents that did not vary with time. At the mean time, perfusion of PhosIQ resulted in significant ($P<0.05$) shifts in the voltage dependence of activation and steady-state inactivation. This included hyperpolarizing shifts of ~20 mV (from

-23.9±0.6 mV; n=5 to -43.7±0.4 mV; n=7) in the midpoints of the normalized sodium conductance curves for activation with noticeable changes in slope (from 6.5±0.4; n=5 to 10.9±0.5 n=6). For steady-state inactivation, there were hyperpolarizing shifts of ~15 mV (from -43.1 mV; n=6 to -59.7 mV; n=8) in the midpoints of the conductance curves. These results indicate a novel mechanism for the regulation of sodium channel current amplitude and the voltage dependence of activation and inactivation kinetics.

The hypothesis regarding regulation of sodium channel kinetics by Ng peptides via a CaM dependent mechanism is surprising, but not unprecedented. CaM appears to be an important regulator of several different ionic currents; recently, Saimi and Kung (2002) proposed that CaM could be considered a channel subunit in itself. The high voltage-activated sodium channels of *Paramecium* are critically dependent on CaM for activation (Saimi and Ling, 1995). CaM has been shown to interact with the C terminus of SK4 potassium channels, and this interaction controls channel assembly and surface expression of SK4 channels (Joiner et al., 2001). Functional expression of KCNQ2/Q3 potassium channels also requires CaM binding, although in this case CaM is not required for targeting of KCNQ2 to the cell membrane despite the fact that KCNQ2 seems to bind CaM constitutively in a calcium-independent manner (Wen and Levitan, 2002). Moreover, Herzog et al. (2003) indicated that disrupting the interaction between CaM and the C-terminus of $Na_V1.4$ and $Na_V1.6$ channels reduced current amplitude by 99 and 62%, respectively.

Although Neurogranin is expressed at relatively high concentrations (~60 μM)

in neuron (Huang et al., 2004), most of them bind calcium-depleted (apo) CaM (20-100 μM) when the intracellular calcium concentration is low (100 nM) at resting. So the free Ng might be below 40 μM, and apoCaM saturated with Ng and other CaM binding proteins. Furthermore, the binding affinity of $Na_v1.3$ to CaM ($K_D \geq 0.1$ μM) is similar to that of Ng to CaM ($K_D \approx 1$ μM), because they both bind CaM with similar IQ motif. Hence, when 100 μM Ng peptide (UnPhosIQ) was infused into cells, a higher Ng concentration results in sharp decrease of CaM available to sodium channel through a "mass action" mechanism (Fig 21.). It is likely that, like $Na_V1.4$ and $Na_V1.6$, disrupting the interaction between CaM and the C-terminus of $Na_V1.3$ channels by Ng peptide may alter channel properties. Previous study (Herzog et al., 2003) showed that CaM could modulate the current amplitude of $Na_V1.4$ and $Na_V1.6$, but not the voltage dependence of activation or inactivation. However, in this study, Ng modulates the Nav1.3 channel properties of activation and inactivation besides current amplitude via CaM. This difference shows that CaM might regulate the properties of VGSCs in isoform-specific ways. The shift in $V_{0.5}$ of activation and steady state inactivation to more depolarize values would ensure that when threshold is reached, there would be an adequate number of channels for action potential initiation and propagation.

In sum, this study is the first time to observe the Ng peptide modulation of the endogenous sodium channels in cortical neuron. Such modulation has potentially interesting implications for the control of neuronal excitability and synaptic transmission by Ng. The Ng-dependent slowing of $Na_v1.3$ inactivation kinetics via CaM could prolong action potential duration.

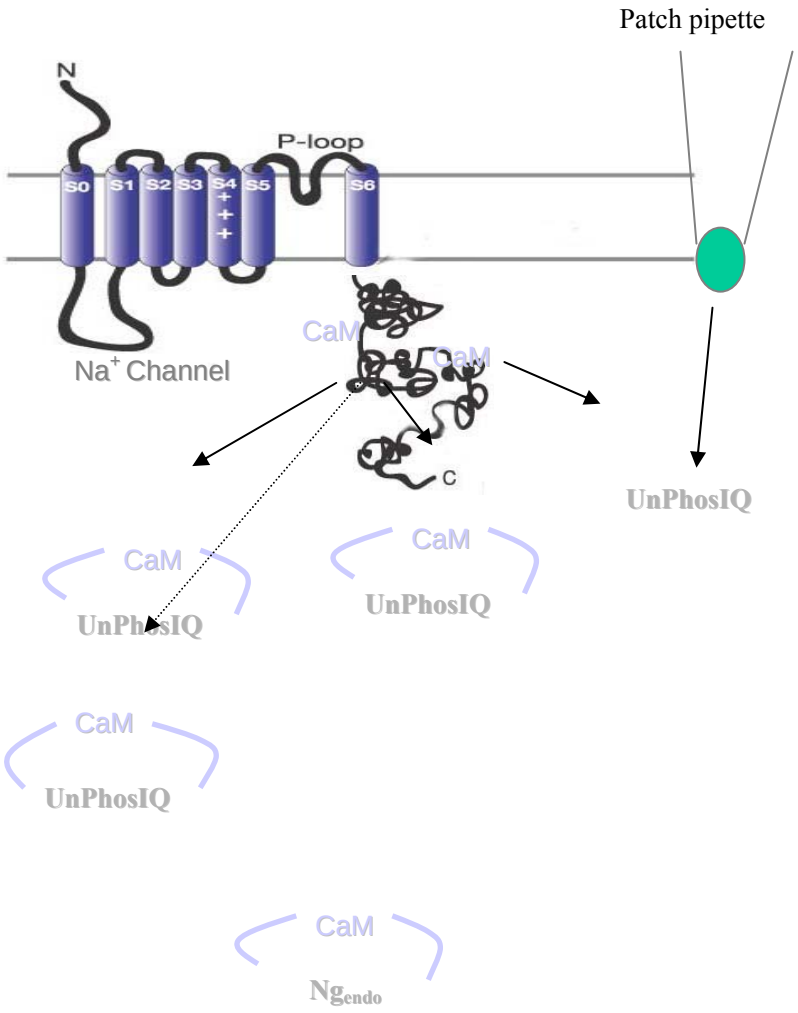

FIG 21. UnPhosIQ mopped up the CaM thus causing the CaM to release from the sodium channel.

4. 2 Ng and CaM at the NMDA channel gate

In this study, we have shown that infusion of Ng peptides, both UnPhosIQ and PhosIQ, results in the slight reduction of Calcium Dependent Inactivation (CDI) of NMDA receptor channels. This result is unexpected. We interpret this type of reduction as a nonspecific action.

According to the molecular model of CDI proposed by Zhang et al. (1998) (see Fig 22), the C terminus of the NR1 subunit is normally anchored to the actin cytoskeleton by its direct interaction with α-actinin2. Upon activation of NMDA receptors, Ca^{2+} influx activates calmodulin and forms Ca_4^{2+}-CaM, which in turn competes with α-actinin2 binding to the C0 region of the NR1 subunit. Calmodulin binding to NR1 would then displace α-actinin2, resulting in the dissociation of the NR1 subunit from the cytoskeleton. The free C terminus of the NR1 subunit may then cause a conformational change in the receptor, or possibly directly interact with other regions of the receptor, thereby decreasing the open probability of the receptor channel (see Figure 22). This model does not involve Ng, though it is a well known modulator of CaM availability in neurons. If this model is correct, let us suppose what would happen if 100 μM Ng peptide, UnphosIQ, was infused into the HEK cell transfected with NMDA receptors. Since there is no endogenous Ng in HEK cell which is human kidney cell, UnPhosIQ may reduce the availability of CaM for CDI by a "mass-action" mechanism; namely, the higher the UnPhosIQ concentration, the more Ng–CaM complexes will be formed, which effectively decrease free CaM at any

given Ca^{2+} influx. On the other hand, Ng peptide accelerates the dissociation of Ca^{2+} from CaM and has little effect on the association rate, which results in decreasing the overall Ca^{2+} binding affinity of the C-domain of CaM. Thus, according to Zhang's model, UnPhosIQ should block CDI significantly, while PhosIQ would not since it cannot bind CaM. However, in this study, both UnPhosIQ and PhosIQ reduce CDI slightly. Why?

In fact, if we pay more attention to the experimental conditions, we will be able to find that the real concentration of free CaM in Hek293 cell is actually very low, only about 1μM. There are two reasons: first, the total concentration of CaM (bound and free) in Hek293 is ~10μM, only half of that in neuron; moreover, according to the amended CDI model proposed by Akyol et al. (2004), the major of these apoCaMs are preassociated with the NMDA receptors by their C domains. These pre-associated CaMs are located in a restricted environment very close to the channel pore and are inaccessible to UnPhosIQ and PhosIQ. In contrast, in this particular experiment, the concentration of two infused Ng peptides (100μM) is much higher than that of the available CaM (free CaM, 1μM). Thus, even PhosIQ, which bind CaM dynamically with low affinity, can also reduce CDI efficiently because of its high concentration (Fig 23).

.

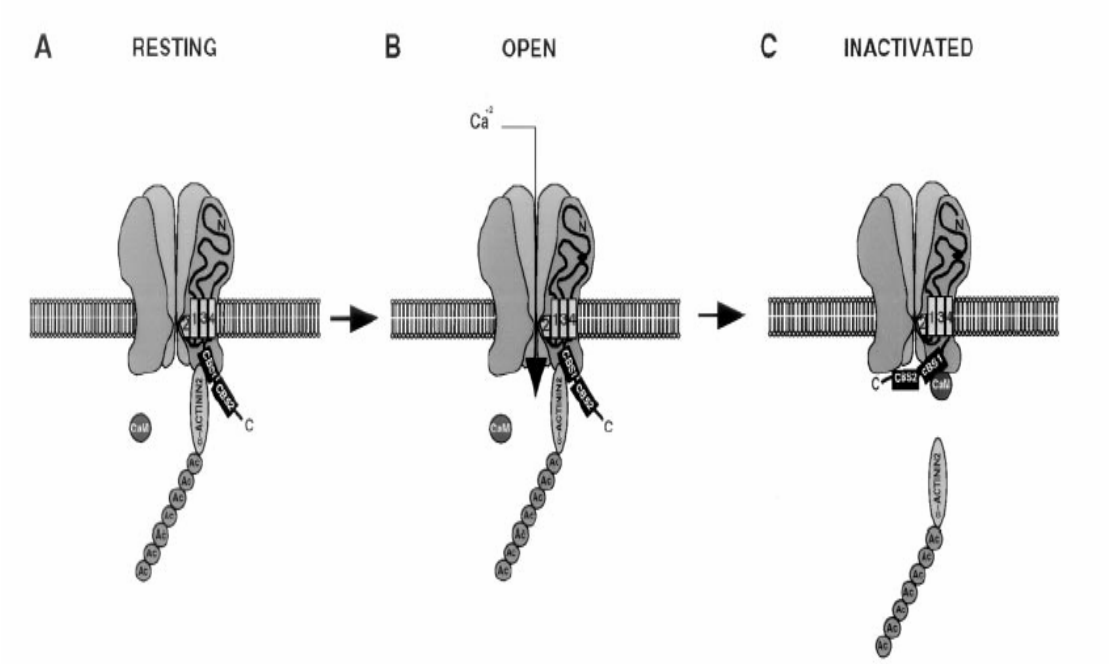

Figure 22. **Schematic Model of CDI**

(A) The CBS1 (within C0) region of the C terminus of the NR1 subunit is normally anchored to the actin cytoskeleton (Ac) by its direct interaction with α-actinin2. (B) Activation of the NMDA receptor increases intracellular Ca^{2+} levels, which then activate calmodulin (CaM). (C) Calmodulin, in turn, competes with α-actinin2 binding to the CBS1 region of the NR1 subunit, resulting in dissociation of the C terminus of the NR1 subunit from the actin cytoskeleton. The free C terminus of the NR1 subunit may then interact with other regions of the NMDA receptor, thereby decreasing the open probability of the receptor channels. (Zhang et al., 1998)

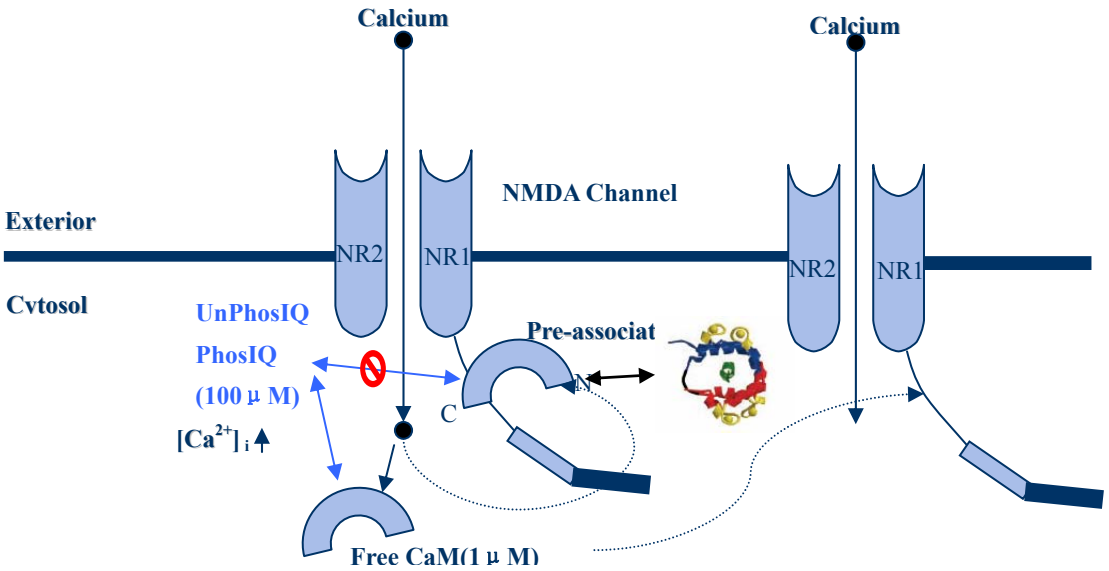

Fig 23. At resting, some of the NMDA receptor channels have been associated with apoCaM (Akyol, 2004), which bind the NR1 C0 region by its C domain. These pre-associated CaMs are located in a restricted environment very close to the channel pore and are inaccessible to UnPhosIQ and PhosIQ. On the other hand, the concentration of two Ng peptides (100 μ M) are much higher than that of the available CaM (free CaM). Thus, even PhosIQ, which bind CaM dynamically with low affinity, can also reduce CDI efficiently.

4.3 Future works

In this study, we used UnPhosIQ, the IQ motif of Ng, as the substitute for whole length Ng because the required high concentration of pure Ng is not available in our lab. We assumed that UnPhosIQ can simulate the behavior of Ng. However, we can not rule out the possibility of the amino acids of Ng outside the IQ motif may contribute to its physiological role and may modulate the binding affinity of Ng for CaM. Thus, further experiments using whole length of Ng protein are indispensable.

In our experiments, we assumed the target protein of UnPhosIQ is CaM. We only have indirect evidence, hence direct methods such as GST pull down, co-immunoprecipitation or yeast two hybrid should be conducted to verify this assumption. In NMDA channel recording experiments, another feasible method is to examine the effect of co-expressing a CaM mutant in which the aspartates in the first position of the four calcium-binding EF hand motifs had been replaced by an alanine to render it calcium-insensitive. This mutant usually is referred to as a dominant-negative form of CaM and is abbreviated as CaM_{1234} (Peterson et al., 1999; (Pitt et al., 2001).

In the study of the sodium channel, all of the experiments were conducted with low intracellular calcium in which the pipette solution contained 5 mM EGTA and 0.5 mM calcium. We wonder whether the Ng regulation of sodium channel could be modulated by changes in intracellular calcium concentration. Thus, more experiments under different intracellular calcium concentration should be conducted.

In the study of NMDA receptor channel, the reason for the nonspecific reduction

of channel CDI may be the high concentration of infused Ng peptides. Thus lower concentration of Ng peptides should be used to see whether there is specific effect of UnPhosIQ infusion. On the other hand, Calcium Dependent Inactivation (CDI) is NR2-subunit specific. The NMDA current amplitudes for NR1/NR2B heteromers are much smaller (100-500pA) than that for NR1/NR2A. Moreover, the CDI of NR1/NR2B is not as evident as that of NR1/NR2A either. Thus, for next step experiments, transfecting the HEK cell with NR1/NR2a heteromers may be a better choice.

4.4 Conclusions

In the current study, we have investigated the roles of Neurogranin peptide in the regulations of both the endogenous sodium channels in cortical neuron and the recombinant NMDA receptor channels in Hek293 cell line. We indicate that the intracellular infusion of an Ng peptide containing unphosphorylated IQ motif substantially modifies the functional properties of sodium channels, while another control peptide containing a phosphorylated IQ motif does not. In contrast, both two Ng peptides can reduce CDI of NMDA receptor channels slightly. It is interesting to see from here, that many still lie in wait for our understanding.

REFERENCE

Anantharam V, Panchal RG, Wilson A, Kolchine VV, Treistman SN, Bayley H (1992) Combinatorial RNA splicing alters the surface charge on the NMDA receptor. FEBS Lett 305:27-30.

Armstrong CM (1981) Sodium channels and gating currents. Physiol Rev 61:644-683.

Ascher P, Nowak L (1988) The role of divalent cations in the N-methyl-D-aspartate responses of mouse central neurones in culture. J Physiol 399:247-266.

Baudier J, Bronner C, Kligman D, Cole RD (1989) Protein kinase C substrates from bovine brain. Purification and characterization of neuromodulin, a neuron-specific calmodulin-binding protein. J Biol Chem 264:1824-1828.

Baudier J, Deloulme JC, Van DA, Black D, Matthes HW (1991) Purification and characterization of a brain-specific protein kinase C substrate, neurogranin (p17). Identification of a consensus amino acid sequence between neurogranin and neuromodulin (GAP43) that corresponds to the protein kinase C phosphorylation site and the calmodulin-binding domain. J Biol Chem 266:229-237.

Bennett MR, Gibson WG, Robinson J (1997) Probabilistic secretion of quanta and the synaptosecretosome hypothesis: evoked release at active zones of varicosities, boutons, and endplates. Biophys J 73:1815-1829.

Benveniste M, Clements J, Vyklicky L, Jr., Mayer ML (1990) A kinetic analysis of the modulation of N-methyl-D-aspartic acid receptors by glycine in mouse cultured hippocampal neurones. J Physiol 428:333-357.

Berridge MJ (1998) Neuronal calcium signaling. Neuron 21:13-26.

Black JA, Cummins TR, Plumpton C, Chen YH, Hormuzdiar W, Clare JJ, Waxman SG (1999) Upregulation of a silent sodium channel after peripheral, but not central, nerve injury in DRG neurons. J Neurophysiol 82:2776-2785.

Bliss TV, Collingridge GL (1993) A synaptic model of memory: long-term potentiation in the hippocampus. Nature 361:31-39.

Bliss TV, Lomo T (1973) Long-lasting potentiation of synaptic transmission in the dentate area of the anaesthetized rabbit following stimulation of the perforant path. J Physiol 232:331-356.

Boiko T, Rasband MN, Levinson SR, Caldwell JH, Mandel G, Trimmer JS, Matthews G (2001) Compact myelin dictates the differential targeting of two sodium channel isoforms in the same axon. Neuron 30:91-104.

Brose N (1993) Membrane fusion takes excitatory turn: syntaxin, vesicle docking protein, or glutamate receptor? Cell 75:1043-1044.

Brose N, Gasic GP, Vetter DE, Sullivan JM, Heinemann SF (1993) Protein chemical characterization and immunocytochemical localization of the NMDA receptor subunit NMDA R1. J Biol Chem 268:22663-22671.

Burgoyne RD, Morgan A (1995) Ca2+ and secretory-vesicle dynamics. Trends Neurosci 18:191-196.

Burnashev N, Schoepfer R, Monyer H, Ruppersberg JP, Gunther W, Seeburg PH, Sakmann B (1992) Control by asparagine residues of calcium permeability and magnesium blockade in the NMDA receptor. Science 257:1415-1419.

Cantrell AR, Catterall WA (2001c) Neuromodulation of Na+ channels: an unexpected form of cellular plasticity. Nat Rev Neurosci 2:397-407.

Cantrell AR, Catterall WA (2001b) Neuromodulation of Na+ channels: an unexpected form of cellular plasticity. Nat Rev Neurosci 2:397-407.

Cantrell AR, Catterall WA (2001a) Neuromodulation of Na+ channels: an unexpected form of cellular plasticity. Nat Rev Neurosci 2:397-407.

Carmignoto G, Vicini S (1992) Activity-dependent decrease in NMDA receptor responses during development of the visual cortex. Science 258:1007-1011.

Catterall WA (2000) From ionic currents to molecular mechanisms: the structure and function of voltage-gated sodium channels. Neuron 26:13-25.

Catterall WA (1986) Molecular properties of voltage-sensitive sodium channels. Annu Rev Biochem 55:953-985.

Cha A, Ruben PC, George AL, Jr., Fujimoto E, Bezanilla F (1999) Voltage sensors in domains III and IV, but not I and II, are immobilized by Na+ channel fast inactivation. Neuron 22:73-87.

Chazot PL, Cik M, Stephenson FA (1992) Immunological detection of the NMDAR1 glutamate receptor subunit expressed in embryonic kidney 293 cells and in rat brain. J Neurochem 59:1176-1178.

Chazot PL, Coleman SK, Cik M, Stephenson FA (1994) Molecular characterization of N-methyl-D-aspartate receptors expressed in mammalian cells yields evidence for the coexistence of three subunit types within a discrete receptor molecule. J Biol Chem 269:24403-24409.

Chin D, Means AR (2000) Calmodulin: a prototypical calcium sensor. Trends Cell Biol 10:322-328.

Choi DW (1988) Glutamate neurotoxicity and diseases of the nervous system. Neuron 1:623-634.

Collingridge GL, Kehl SJ, McLennan H (1983) Excitatory amino acids in synaptic transmission in the Schaffer collateral-commissural pathway of the rat hippocampus. J Physiol 334:33-46.

Davies J, Francis AA, Jones AW, Watkins JC (1981) 2-Amino-5-phosphonovalerate (2APV), a potent and selective antagonist of amino acid-induced and synaptic excitation. Neurosci Lett 21:77-81.

Davis S, Butcher SP, Morris RG (1992) The NMDA receptor antagonist D-2-amino-5-phosphonopentanoate (D-AP5) impairs spatial learning and LTP in vivo at intracerebral concentrations comparable to those that block LTP in vitro. J Neurosci 12:21-34.

Doyle DA, Morais CJ, Pfuetzner RA, Kuo A, Gulbis JM, Cohen SL, Chait BT, MacKinnon R (1998) The structure of the potassium channel: molecular basis of K+ conduction and selectivity. Science 280:69-77.

Durand GM, Gregor P, Zheng X, Bennett MV, Uhl GR, Zukin RS (1992) Cloning of an apparent splice variant of the rat N-methyl-D-aspartate receptor NMDAR1 with altered sensitivity to polyamines and activators of protein kinase C. Proc Natl Acad Sci U S A 89:9359-9363.

Eaholtz G, Scheuer T, Catterall WA (1994) Restoration of inactivation and block of open sodium channels by an inactivation gate peptide. Neuron 12:1041-1048.

Ehlers MD, Zhang S, Bernhadt JP, Huganir RL (1996) Inactivation of NMDA receptors by direct interaction of calmodulin with the NR1 subunit. Cell 84:745-755.

Emptage NJ, Reid CA, Fine A (2001) Calcium stores in hippocampal synaptic boutons mediate short-term plasticity, store-operated Ca2+ entry, and spontaneous transmitter release. Neuron 29:197-208.

Gerendasy DD, Herron SR, Jennings PA, Sutcliffe JG (1995) Calmodulin stabilizes an amphiphilic alpha-helix within RC3/neurogranin and GAP-43/neuromodulin only when Ca2+ is absent. J Biol Chem 270:6741-6750.

Gerendasy DD, Herron SR, Watson JB, Sutcliffe JG (1994) Mutational and biophysical studies suggest RC3/neurogranin regulates calmodulin availability. J Biol Chem 269:22420-22426.

Gerendasy DD, Sutcliffe JG (1997) RC3/neurogranin, a postsynaptic calpacitin for setting the response threshold to calcium influxes. Mol Neurobiol 15:131-163.

Grenningloh G, Rienitz A, Schmitt B, Methfessel C, Zensen M, Beyreuther K,

Gundelfinger ED, Betz H (1987) The strychnine-binding subunit of the glycine receptor shows homology with nicotinic acetylcholine receptors. Nature 328:215-220.

Guy HR, Seetharamulu P (1986) Molecular model of the action potential sodium channel. Proc Natl Acad Sci U S A 83:508-512.

Heinemann SH, Terlau H, Stuhmer W, Imoto K, Numa S (1992) Calcium channel characteristics conferred on the sodium channel by single mutations. Nature 356:441-443.

Herzog RI, Liu C, Waxman SG, Cummins TR (2003) Calmodulin binds to the C terminus of sodium channels Nav1.4 and Nav1.6 and differentially modulates their functional properties. J Neurosci 23:8261-8270.

Hestrin S (1992) Developmental regulation of NMDA receptor-mediated synaptic currents at a central synapse. Nature 357:686-689.

Hilborn MD, Vaillancourt RR, Rane SG (1998) Growth factor receptor tyrosine kinases acutely regulate neuronal sodium channels through the src signaling pathway. J Neurosci 18:590-600.

Hodgkin AL, Huxley AF (1952a) A quantitative description of membrane current and its application to conduction and excitation in nerve. J Physiol 117:500-544.

Hollmann M, Boulter J, Maron C, Beasley L, Sullivan J, Pecht G, Heinemann S (1993) Zinc potentiates agonist-induced currents at certain splice variants of the NMDA receptor. Neuron 10:943-954.

Huang KP, Huang FL, Chen HC (1993b) Characterization of a 7.5-kDa protein kinase C substrate (RC3 protein, neurogranin) from rat brain. Arch Biochem Biophys 305:570-580.

Huang KP, Huang FL, Chen HC (1993a) Characterization of a 7.5-kDa protein kinase C substrate (RC3 protein, neurogranin) from rat brain. Arch Biochem Biophys 305:570-580.

Huang KP, Huang FL, Jager T, Li J, Reymann KG, Balschun D (2004) Neurogranin/RC3 enhances long-term potentiation and learning by promoting calcium-mediated signaling. J Neurosci 24:10660-10669.

Ikeda K, Nagasawa M, Mori H, Araki K, Sakimura K, Watanabe M, Inoue Y, Mishina M (1992a) Cloning and expression of the epsilon 4 subunit of the NMDA receptor channel. FEBS Lett 313:34-38.

Ikeda K, Nagasawa M, Mori H, Araki K, Sakimura K, Watanabe M, Inoue Y, Mishina M (1992b) Cloning and expression of the epsilon 4 subunit of the NMDA receptor channel. FEBS Lett 313:34-38.

Ishii T, Moriyoshi K, Sugihara H, Sakurada K, Kadotani H, Yokoi M, Akazawa C, Shigemoto R, Mizuno N, Masu M, . (1993b) Molecular characterization of the family of the N-methyl-D-aspartate receptor subunits. J Biol Chem 268:2836-2843.

Ishii T, Moriyoshi K, Sugihara H, Sakurada K, Kadotani H, Yokoi M, Akazawa C, Shigemoto R, Mizuno N, Masu M, . (1993a) Molecular characterization of the family of the N-methyl-D-aspartate receptor subunits. J Biol Chem 268:2836-2843.

Johnson JW, Ascher P (1987b) Glycine potentiates the NMDA response in cultured mouse brain neurons. Nature 325:529-531.

Johnson JW, Ascher P (1987a) Glycine potentiates the NMDA response in cultured mouse brain neurons. Nature 325:529-531.

Joiner WJ, Khanna R, Schlichter LC, Kaczmarek LK (2001) Calmodulin regulates assembly and trafficking of SK4/IK1 Ca2+-activated K+ channels. J Biol Chem 276:37980-37985.

Kaplan MR, Cho MH, Ullian EM, Isom LL, Levinson SR, Barres BA (2001) Differential control of clustering of the sodium channels Na(v)1.2 and Na(v)1.6 at developing CNS nodes of Ranvier. Neuron 30:105-119.

Kellenberger S, Scheuer T, Catterall WA (1996) Movement of the Na+ channel inactivation gate during inactivation. J Biol Chem 271:30971-30979.

Krupp JJ, Vissel B, Thomas CG, Heinemann SF, Westbrook GL (1999) Interactions of calmodulin and alpha-actinin with the NR1 subunit modulate Ca2+-dependent inactivation of NMDA receptors. J Neurosci 19:1165-1178.

Kuryatov A, Laube B, Betz H, Kuhse J (1994) Mutational analysis of the glycine-binding site of the NMDA receptor: structural similarity with bacterial amino acid-binding proteins. Neuron 12:1291-1300.

Kutsuwada T, Kashiwabuchi N, Mori H, Sakimura K, Kushiya E, Araki K, Meguro H, Masaki H, Kumanishi T, Arakawa M, . (1992b) Molecular diversity of the NMDA receptor channel. Nature 358:36-41.

Kutsuwada T, Kashiwabuchi N, Mori H, Sakimura K, Kushiya E, Araki K, Meguro H, Masaki H, Kumanishi T, Arakawa M, . (1992a) Molecular diversity of the NMDA receptor channel. Nature 358:36-41.

Laurie DJ, Seeburg PH (1994) Regional and developmental heterogeneity in splicing of the rat brain NMDAR1 mRNA. J Neurosci 14:3180-3194.

Lee SH, Kim MC, Heo WD, Kim JC, Chung WS, Park CY, Park HC, Cheong YH, Kim CY, Lee KJ, Bahk JD, Lee SY, Cho MJ (1999) Competitive binding of calmodulin isoforms to calmodulin-binding proteins: implication for the function of

calmodulin isoforms in plants. Biochim Biophys Acta 1433:56-67.

Legendre P, Rosenmund C, Westbrook GL (1993) Inactivation of NMDA channels in cultured hippocampal neurons by intracellular calcium. J Neurosci 13:674-684.

Lester RA, Jahr CE (1992) NMDA channel behavior depends on agonist affinity. J Neurosci 12:635-643.

Levitan IB (1999) It is calmodulin after all! Mediator of the calcium modulation of multiple ion channels. Neuron 22:645-648.

Li S, Huang FL, Feng Q, Liu J, Fan SX, McKenna TM (1998) Overexpression of protein kinase C alpha enhances lipopolysaccharide-induced nitric oxide formation in vascular smooth muscle cells. J Cell Physiol 176:402-411.

Ling KY, Preston RR, Burns R, Kink JA, Saimi Y, Kung C (1992) Primary mutations in calmodulin prevent activation of the Ca(++)-dependent Na+ channel in Paramecium. Proteins 12:365-371.

Liu YC, Storm DR (1990) Regulation of free calmodulin levels by neuromodulin: neuron growth and regeneration. Trends Pharmacol Sci 11:107-111.

Ma JY, Catterall WA, Scheuer T (1997) Persistent sodium currents through brain sodium channels induced by G protein betagamma subunits. Neuron 19:443-452.

MacDermott AB, Mayer ML, Westbrook GL, Smith SJ, Barker JL (1986) NMDA-receptor activation increases cytoplasmic calcium concentration in cultured spinal cord neurones. Nature 321:519-522.

Malenka RC, Nicoll RA (1993) NMDA-receptor-dependent synaptic plasticity: multiple forms and mechanisms. Trends Neurosci 16:521-527.

Mayer ML, Vyklicky L, Jr., Clements J (1989) Regulation of NMDA receptor desensitization in mouse hippocampal neurons by glycine. Nature 338:425-427.

Mayer ML, Westbrook GL (1985) The action of N-methyl-D-aspartic acid on mouse spinal neurones in culture. J Physiol 361:65-90.

Mayer ML, Westbrook GL (1987) Permeation and block of N-methyl-D-aspartic acid receptor channels by divalent cations in mouse cultured central neurones. J Physiol 394:501-527.

Meguro H, Mori H, Araki K, Kushiya E, Kutsuwada T, Yamazaki M, Kumanishi T, Arakawa M, Sakimura K, Mishina M (1992b) Functional characterization of a heteromeric NMDA receptor channel expressed from cloned cDNAs. Nature 357:70-74.

Meguro H, Mori H, Araki K, Kushiya E, Kutsuwada T, Yamazaki M, Kumanishi T,

Arakawa M, Sakimura K, Mishina M (1992a) Functional characterization of a heteromeric NMDA receptor channel expressed from cloned cDNAs. Nature 357:70-74.

Meyer T, Hanson PI, Stryer L, Schulman H (1992) Calmodulin trapping by calcium-calmodulin-dependent protein kinase. Science 256:1199-1202.

Mishina M, Mori H, Araki K, Kushiya E, Meguro H, Kutsuwada T, Kashiwabuchi N, Ikeda K, Nagasawa M, Yamazaki M, . (1993a) Molecular and functional diversity of the NMDA receptor channel. Ann N Y Acad Sci 707:136-152.

Mishina M, Mori H, Araki K, Kushiya E, Meguro H, Kutsuwada T, Kashiwabuchi N, Ikeda K, Nagasawa M, Yamazaki M, . (1993b) Molecular and functional diversity of the NMDA receptor channel. Ann N Y Acad Sci 707:136-152.

Monyer H, Burnashev N, Laurie DJ, Sakmann B, Seeburg PH (1994) Developmental and regional expression in the rat brain and functional properties of four NMDA receptors. Neuron 12:529-540.

Monyer H, Sprengel R, Schoepfer R, Herb A, Higuchi M, Lomeli H, Burnashev N, Sakmann B, Seeburg PH (1992b) Heteromeric NMDA receptors: molecular and functional distinction of subtypes. Science 256:1217-1221.

Monyer H, Sprengel R, Schoepfer R, Herb A, Higuchi M, Lomeli H, Burnashev N, Sakmann B, Seeburg PH (1992a) Heteromeric NMDA receptors: molecular and functional distinction of subtypes. Science 256:1217-1221.

Mori H, Yamakura T, Masaki H, Mishina M (1993) Involvement of the carboxyl-terminal region in modulation by TPA of the NMDA receptor channel. Neuroreport 4:519-522.

Moriyoshi K, Masu M, Ishii T, Shigemoto R, Mizuno N, Nakanishi S (1991b) Molecular cloning and characterization of the rat NMDA receptor. Nature 354:31-37.

Moriyoshi K, Masu M, Ishii T, Shigemoto R, Mizuno N, Nakanishi S (1991a) Molecular cloning and characterization of the rat NMDA receptor. Nature 354:31-37.

Morris RG, Anderson E, Lynch GS, Baudry M (1986) Selective impairment of learning and blockade of long-term potentiation by an N-methyl-D-aspartate receptor antagonist, AP5. Nature 319:774-776.

Nakanishi N, Axel R, Shneider NA (1992) Alternative splicing generates functionally distinct N-methyl-D-aspartate receptors. Proc Natl Acad Sci U S A 89:8552-8556.

Noda M, Suzuki H, Numa S, Stuhmer W (1989) A single point mutation confers tetrodotoxin and saxitoxin insensitivity on the sodium channel II. FEBS Lett 259:213-216.

Noda M, Takahashi H, Tanabe T, Toyosato M, Kikyotani S, Furutani Y, Hirose T, Takashima H, Inayama S, Miyata T, Numa S (1983) Structural homology of Torpedo californica acetylcholine receptor subunits. Nature 302:528-532.

Nowak L, Bregestovski P, Ascher P, Herbet A, Prochiantz A (1984) Magnesium gates glutamate-activated channels in mouse central neurones. Nature 307:462-465.

Olney JW (1990) Excitotoxic amino acids and neuropsychiatric disorders. Annu Rev Pharmacol Toxicol 30:47-71.

Pak JH, Huang FL, Li J, Balschun D, Reymann KG, Chiang C, Westphal H, Huang KP (2000) Involvement of neurogranin in the modulation of calcium/calmodulin-dependent protein kinase II, synaptic plasticity, and spatial learning: a study with knockout mice. Proc Natl Acad Sci U S A 97:11232-11237.

Parsons CG, Zong X, Lux HD (1993) Whole cell and single channel analysis of the kinetics of glycine-sensitive N-methyl-D-aspartate receptor desensitization. Br J Pharmacol 109:213-221.

Perkel DJ, Hestrin S, Sah P, Nicoll RA (1990) Excitatory synaptic currents in Purkinje cells. Proc Biol Sci 241:116-121.

Peterson BZ, DeMaria CD, Adelman JP, Yue DT (1999) Calmodulin is the Ca2+ sensor for Ca2+ -dependent inactivation of L-type calcium channels. Neuron 22:549-558.

Pitt GS, Zuhlke RD, Hudmon A, Schulman H, Reuter H, Tsien RW (2001) Molecular basis of calmodulin tethering and Ca2+-dependent inactivation of L-type Ca2+ channels. J Biol Chem 276:30794-30802.

Prichard L, Deloulme JC, Storm DR (1999) Interactions between neurogranin and calmodulin in vivo. J Biol Chem 274:7689-7694.

Quinlan JE, Davies J (1985) Excitatory and inhibitory responses of Purkinje cells, in the rat cerebellum in vivo, induced by excitatory amino acids. Neurosci Lett 60:39-46.

Ratcliffe CF, Qu Y, McCormick KA, Tibbs VC, Dixon JE, Scheuer T, Catterall WA (2000) A sodium channel signaling complex: modulation by associated receptor protein tyrosine phosphatase beta. Nat Neurosci 3:437-444.

Ren D, Navarro B, Xu H, Yue L, Shi Q, Clapham DE (2001) A prokaryotic voltage-gated sodium channel. Science 294:2372-2375.

Rohl CA, Boeckman FA, Baker C, Scheuer T, Catterall WA, Klevit RE (1999) Solution structure of the sodium channel inactivation gate. Biochemistry 38:855-861.

Saimi Y, Kung C (2002) Calmodulin as an ion channel subunit. Annu Rev Physiol

64:289-311.

Saimi Y, Ling KY (1995) Paramecium Na+ channels activated by Ca(2+)-calmodulin: calmodulin is the Ca2+ sensor in the channel gating mechanism. J Membr Biol 144:257-265.

Sakimura K, Kutsuwada T, Ito I, Manabe T, Takayama C, Kushiya E, Yagi T, Aizawa S, Inoue Y, Sugiyama H, . (1995) Reduced hippocampal LTP and spatial learning in mice lacking NMDA receptor epsilon 1 subunit. Nature 373:151-155.

Sather W, Johnson JW, Henderson G, Ascher P (1990) Glycine-insensitive desensitization of NMDA responses in cultured mouse embryonic neurons. Neuron 4:725-731.

Sato C, Ueno Y, Asai K, Takahashi K, Sato M, Engel A, Fujiyoshi Y (2001) The voltage-sensitive sodium channel is a bell-shaped molecule with several cavities. Nature 409:1047-1051.

Schlief T, Schonherr R, Imoto K, Heinemann SH (1996) Pore properties of rat brain II sodium channels mutated in the selectivity filter domain. Eur Biophys J 25:75-91.

Schultz J, Copley RR, Doerks T, Ponting CP, Bork P (2000) SMART: a web-based tool for the study of genetically mobile domains. Nucleic Acids Res 28:231-234.

Seeburg PH (1993) The TINS/TiPS Lecture. The molecular biology of mammalian glutamate receptor channels. Trends Neurosci 16:359-365.

Sheng M, Cummings J, Roldan LA, Jan YN, Jan LY (1994a) Changing subunit composition of heteromeric NMDA receptors during development of rat cortex. Nature 368:144-147.

Sheng M, Cummings J, Roldan LA, Jan YN, Jan LY (1994b) Changing subunit composition of heteromeric NMDA receptors during development of rat cortex. Nature 368:144-147.

Sheng M, Cummings J, Roldan LA, Jan YN, Jan LY (1994c) Changing subunit composition of heteromeric NMDA receptors during development of rat cortex. Nature 368:144-147.

Sheu FS, Mahoney CW, Seki K, Huang KP (1996) Nitric oxide modification of rat brain neurogranin affects its phosphorylation by protein kinase C and affinity for calmodulin. J Biol Chem 271:22407-22413.

Standaert DG, Testa CM, Young AB, Penney JB, Jr. (1994) Organization of N-methyl-D-aspartate glutamate receptor gene expression in the basal ganglia of the rat. J Comp Neurol 343:1-16.

Stemmer PM, Klee CB (1994) Dual calcium ion regulation of calcineurin by calmodulin and calcineurin B. Biochemistry 33:6859-6866.

Stuhmer W, Conti F, Suzuki H, Wang XD, Noda M, Yahagi N, Kubo H, Numa S (1989) Structural parts involved in activation and inactivation of the sodium channel. Nature 339:597-603.

Sugihara H, Moriyoshi K, Ishii T, Masu M, Nakanishi S (1992) Structures and properties of seven isoforms of the NMDA receptor generated by alternative splicing. Biochem Biophys Res Commun 185:826-832.

Sullivan JM, Traynelis SF, Chen HS, Escobar W, Heinemann SF, Lipton SA (1994) Identification of two cysteine residues that are required for redox modulation of the NMDA subtype of glutamate receptor. Neuron 13:929-936.

Tan HL, Kupershmidt S, Zhang R, Stepanovic S, Roden DM, Wilde AA, Anderson ME, Balser JR (2002) A calcium sensor in the sodium channel modulates cardiac excitability. Nature 415:442-447.

Tingley WG, Roche KW, Thompson AK, Huganir RL (1993) Regulation of NMDA receptor phosphorylation by alternative splicing of the C-terminal domain. Nature 364:70-73.

Toledo-Aral JJ, Moss BL, He ZJ, Koszowski AG, Whisenand T, Levinson SR, Wolf JJ, Silos-Santiago I, Halegoua S, Mandel G (1997) Identification of PN1, a predominant voltage-dependent sodium channel expressed principally in peripheral neurons. Proc Natl Acad Sci U S A 94:1527-1532.

Vassilev P, Scheuer T, Catterall WA (1989) Inhibition of inactivation of single sodium channels by a site-directed antibody. Proc Natl Acad Sci U S A 86:8147-8151.

Watanabe M, Inoue Y, Sakimura K, Mishina M (1993) Distinct distributions of five N-methyl-D-aspartate receptor channel subunit mRNAs in the forebrain. J Comp Neurol 338:377-390.

Watanabe M, Inoue Y, Sakimura K, Mishina M (1992) Developmental changes in distribution of NMDA receptor channel subunit mRNAs. Neuroreport 3:1138-1140.

Watanabe M, Mishina M, Inoue Y (1994a) Distinct spatiotemporal expressions of five NMDA receptor channel subunit mRNAs in the cerebellum. J Comp Neurol 343:513-519.

Watanabe M, Mishina M, Inoue Y (1994b) Distinct distributions of five NMDA receptor channel subunit mRNAs in the brainstem. J Comp Neurol 343:520-531.

Watkins WM, Hassid WZ (1962) The synthesis of lactose by particulate enzyme preparations from guinea pig and bovine mammary glands. J Biol Chem

237:1432-1440.

Watson JB, Battenberg EF, Wong KK, Bloom FE, Sutcliffe JG (1990) Subtractive cDNA cloning of RC3, a rodent cortex-enriched mRNA encoding a novel 78 residue protein. J Neurosci Res 26:397-408.

Watson JB, Sutcliffe JG, Fisher RS (1992) Localization of the protein kinase C phosphorylation/calmodulin-binding substrate RC3 in dendritic spines of neostriatal neurons. Proc Natl Acad Sci U S A 89:8581-8585.

Wen H, Levitan IB (2002) Calmodulin is an auxiliary subunit of KCNQ2/3 potassium channels. J Neurosci 22:7991-8001.

Westenbroek RE, Merrick DK, Catterall WA (1989) Differential subcellular localization of the RI and RII Na+ channel subtypes in central neurons. Neuron 3:695-704.

Wo ZG, Oswald RE (1995) Unraveling the modular design of glutamate-gated ion channels. Trends Neurosci 18:161-168.

Wyszynski M, Lin J, Rao A, Nigh E, Beggs AH, Craig AM, Sheng M (1997) Competitive binding of alpha-actinin and calmodulin to the NMDA receptor. Nature 385:439-442.

Yamazaki M, Mori H, Araki K, Mori KJ, Mishina M (1992a) Cloning, expression and modulation of a mouse NMDA receptor subunit. FEBS Lett 300:39-45.

Yamazaki M, Mori H, Araki K, Mori KJ, Mishina M (1992b) Cloning, expression and modulation of a mouse NMDA receptor subunit. FEBS Lett 300:39-45.

Yang N, George AL, Jr., Horn R (1996) Molecular basis of charge movement in voltage-gated sodium channels. Neuron 16:113-122.

Yang N, Horn R (1995) Evidence for voltage-dependent S4 movement in sodium channels. Neuron 15:213-218.

Zhang S, Ehlers MD, Bernhardt JP, Su CT, Huganir RL (1998) Calmodulin mediates calcium-dependent inactivation of N-methyl-D-aspartate receptors. Neuron 21:443-453.

Zuhlke RD, Pitt GS, Deisseroth K, Tsien RW, Reuter H (1999) Calmodulin supports both inactivation and facilitation of L-type calcium channels. Nature 399:159-162.